Catalytic Oxygen Atom Transfer Through Photochemical and Electrochemical Activation of O2 or H2O

Elena A Tacchi, Elodie Anxolabéhère-mallart, Ally Aukauloo, Claire Fave, Marc Robert, Andrea Sartorel

Angewandte Novit Chemie

Minireview
DOI:10.1002/anov.70007

GDCh German Chemical Society

Catalytic Oxygen Atom Transfer Through Photochemical and Electrochemical Activation of O_2 or H_2O

*Elena Tacchi, Elodie Anxolabéhère-Mallart, Ally Aukauloo, Claire Fave, Marc Robert, and Andrea Sartorel**

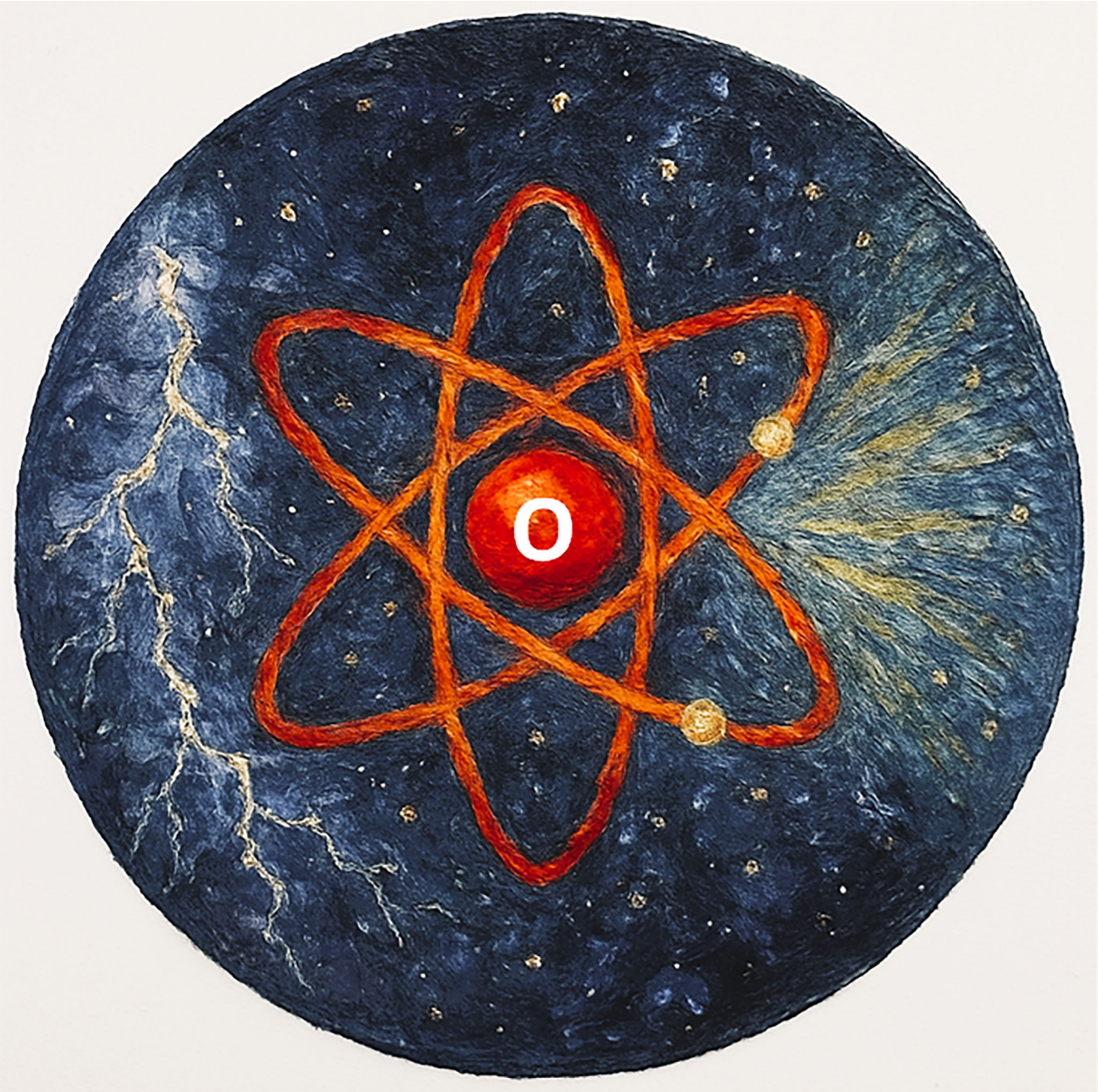

Angewandte Novit Chemie

Abstract: Chemical transformations involving oxygen atom transfer (OAT) to organic substrates attract significant interest across industrial, pharmaceutical, and fundamental chemical research, including areas such as bioinorganic chemistry, catalysis, and synthetic methodology. Recent advances in electrochemical and photochemical catalysis have opened up new pathways for enabling OAT processes, particularly through the reductive activation of dioxygen or oxidative activation of water. This minireview explores emerging approaches in the field, including electrocatalytic methods leveraging bioinspired transition metal complexes, photocatalytic platforms integrating catalysts with photosensitizers, photoactive materials, or organic photocatalysts, and hybrid methodologies combining electrochemical and photochemical activation. We outline future directions for innovation, ranging from the design of functional molecular architectures and device engineering to the development of scalable technologies for industrial applications.

1. Introduction

Many chemical processes must be reconsidered, and new, more sustainable technologies are essential for a greener future. This is especially true for oxygen atom transfer (OAT), which involves inserting an oxygen atom into an organic substrate. OAT is highly significant in both industry[1] and pharmaceuticals,[2] particularly for large-scale production of important chemicals and intermediates. Two of the most challenging OAT reactions are the epoxidation of C═C double bonds and the hydroxylation of C─H bonds (Scheme 1, panel A). In industrial settings, these oxidation processes are primarily carried out via radical-based mechanisms. However, such approaches face limitations, particularly in controlling selectivity—especially to prevent over-oxidation—and in activating more challenging substrates.

Epoxidation is widely used industrially, such as in converting ethylene to ethylene oxide (34 million metric tons in 2021) and propylene to propylene oxide (10 million tons in 2014). Ethylene oxide is produced using O_2 and silver-based catalysts, achieving conversion and selectivity rates of up to 90%.[3,4] The resulting crude product mixture is then further processed, for example by reacting with water, to produce ethylene glycol as one of the downstream products.[3,4] Propylene oxide synthesis is more difficult due to the high reactivity of allylic hydrogens, resulting in limited selectivity even at low conversion (60%–80% selectivity at <3% conversion with silver catalysts operating via radical mechanism[1]). Thus, direct propylene epoxidation remains an aspirational goal.

Hydroxylation of C─H bonds becomes more difficult as bond strength increases, measured by bond dissociation

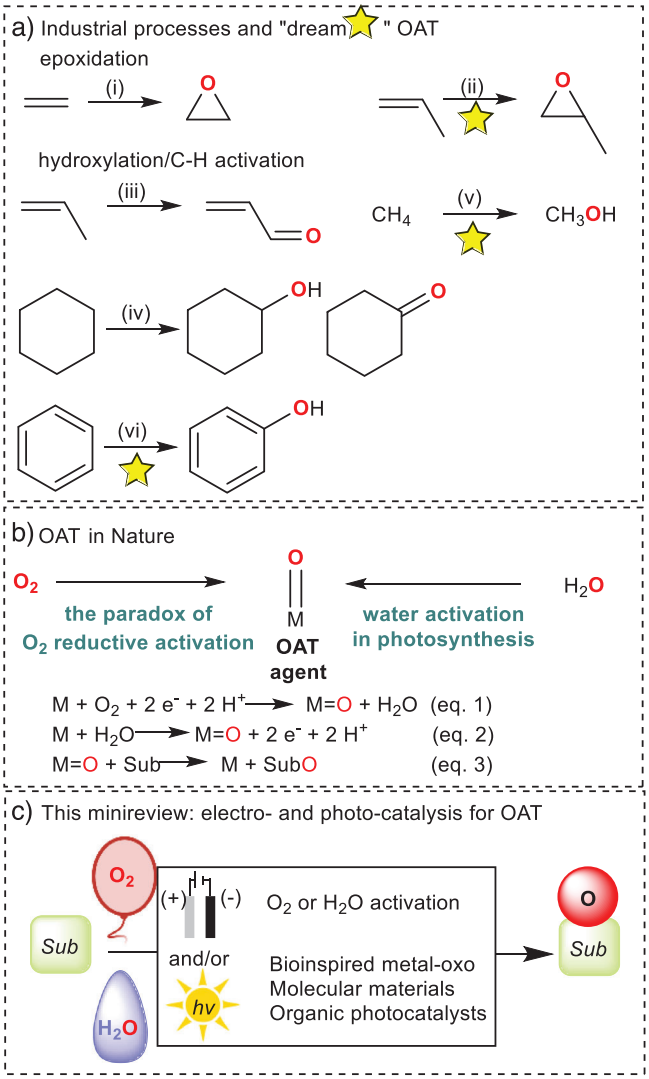

Scheme 1. a) Industrial and dream OAT processes. Industrial conditions: (i) O_2 (5%–9% vol%), Ag/α-Al_2O_3 catalyst, 210°–280 °C, 10–20 atm; (ii) several procedures with Cl_2, H_2O_2, and organic hydroperoxides; (iii) O_2 and Bi_2O_3·MoO_3 multicomponent catalysts; (iv) air, Co catalyst T 145–160°C, P 8–20 atm; (v) steam reforming process coupled with catalysis by CuO/ZnO/Al_2O_3; (vi) N_2O, Fe-ZSM-5. b) Generation of metal-oxo OAT agents through O_2 or water activation in nature. c) Presentation of this minireview.

[*] E. Tacchi, Prof. A. Sartorel
Department of Chemical Sciences, University of Padova, via Marzolo 1, Padova 35131, Italy
E-mail: andrea.sartorel@unipd.it

Dr. E. Anxolabéhère-Mallart, Dr. C. Fave, Prof. M. Robert
Sorbonne Université, CNRS, Institut Parisien de Chimie Moléculaire, IPCM, Paris F-75005, France

Prof. A. Aukauloo
ICMMO UMR 8182, Université Paris-Saclay, Bâtiment 670, 17–19 Avenue des Sciences, Orsay 91400, France

free energy (BDFE).[5] Industrially, *p*-terephthalic acid is produced by oxidizing *p*-xylene in >95% yield,[6] and acrolein (5 Mtons in 2014) is made from propylene oxidation (90% selectivity at >95% conversion), both involving activated benzylic and allylic C─H bonds and exploiting catalytic, radical based aerobic processes. More demanding is the oxidation of cyclohexane (BDFE ≈ 95 kcal·mol^{-1}) to cyclohexanol and cyclohexanone (KA oil), key precursors for adipic acid and ε-caprolactam, used in nylon production. This process, using air and a cobalt catalyst, suffers from low selectivity (70%–80% at 4%–5% conversion) and high energy use.[7] The ultimate goals in OAT hydroxylation are methane to methanol[8] and benzene to phenol conversions. For phenol, a pilot process used N_2O and Fe-doped ZSM-5 zeolite (Scheme 1a), while in industrial manufacturing, the process is based on the aerobic oxidation of cumene via a radical mechanism, proceeding through a cumene hydroperoxide intermediate. Overall, advancing sustainable OAT methods is crucial for greener chemical manufacturing, yet significant challenges remain in achieving efficient and selective transformations for key industrial targets.

In this context, there is a growing focus on developing sustainable approaches to directly oxygenate C─H and C═C bonds. These methods leverage molecular oxygen or water—Earth's most abundant oxygen atom sources—with natural systems serving as the primary blueprint. In biological systems, OAT occurs through metalloenzymes that generate various key intermediates as high-valent metal-oxo species (M═O, Scheme 1b). These M═O compounds are the active agents responsible for oxygen transfer. Notably, the activation mechanisms for O_2 and H_2O follow fundamentally different pathways. Monooxygenase enzymes, such as cytochrome P450,[9–11] demonstrate a fascinating capability: they activate molecular oxygen even while requiring reducing equivalents. This seeming contradiction enables these enzymes to split the O_2 molecule, ultimately generating a heme Fe^{IV}═O intermediate (known as Compound I, bearing a radical cation on the porphyrin ring) that performs the oxygen transfer, with water formed as a byproduct (Equation 1 in Scheme 1b). In contrast, dioxygenase enzymes employ a different strategy, incorporating both oxygen atoms from the O_2 molecule directly into the substrate. Unlike oxygen, water requires oxidative activation to form metal-oxo species. The tetramanganese oxygen-evolving center exemplifies this process, playing a crucial role in water oxidation. Natural systems transform water into O_2 through complete four-electron, four-proton oxidation. However, researchers have proposed reconceptualizing this mechanism as a partial two-electron, two-proton oxidation, subsequently followed by OAT to the substrate (Equations 2 and 3 in Scheme 1b).

Drawing inspiration from these biological systems, researchers have developed synthetic analogs of natural metal-oxo complexes. These synthetic models primarily utilize first-row transition metals from the d-block, including iron, manganese, cobalt and copper—though notably, cobalt, and copper technically exist beyond what's known as the "oxo-wall"[12] in coordination chemistry.[13–15] Examples of bioinspired synthetic metal-oxo key intermediates were reported, among others, by Gray,[16] Que,[17] Groves,[18,19] Nam and Fukuzumi,[20,21] Collins,[22,23] Costas and Fillol[24] and Kojima.[8] However, most of the synthetic M═O analogs perform OAT in the presence of chemical oxidants acting as oxygen atom donors, while examples of direct O_2 activation are rare.[25,26]

The resurgence of electrochemical and photochemical catalytic approaches presents innovative pathways for facilitating OAT through the activation of O_2 or H_2O. These methodologies-whether applied individually or in synergistic combination-share a fundamental advantage: they enable the transaction of electrons without introducing chemical residues, effectively serving as "traceless reagents." This clean electron transfer capability proves crucial for generating the active species that ultimately perform OAT reactions.

These opportunities are reported in this minireview (Scheme 1c). Specifically, the second section examines electrochemical approaches where metal complex activation produces bioinspired metal-oxo species functioning as OAT agents, utilizing either O_2 or H_2O as the oxygen source. The third section focuses on photochemical systems where light energy drives the formation of OAT agents, primarily through combinations of photosensitizers with molecular metal complexes. This fundamental understanding of component interactions has enabled the development of scalable photoactive materials. Finally, the fourth section explores alternative activation pathways for O_2 and water, highlighting photochemical and photoelectrochemical systems incorporating organic photoactive components that operate through distinct mechanistic routes. In the examples discussed in this review, we focused mainly on activation of bioinspired metal complexes and on the use of organic photocatalysts; we did not include cases where singlet oxygen ($^1O_2$), ·OH, $O_2^{\bullet-}$, H_2O_2, HOCl, halogen, and oxynitride radicals operate as key intermediates; nevertheless, we comment on this alternative approach in the Summary and Outlook section.

Besides the operating conditions (experimental conditions, product yield, and productivity), the evaluation of an electro- or photocatalytic process may also include catalytic key performance indicators, such as turnover number (TON), turnover frequency (TOF), Faradaic yield (FY, for electrochemical systems), and quantum yield (ϕ, for photochemical systems). Comparison of performances between different systems, even related ones, is often hampered by calculation hypotheses and significantly different experimental conditions in which they were evaluated. Our aim is not to provide an extensive review nor a thorough discussion of the metrics related to the growing number of examples reported, but rather to point to the strategies chemists are seeking to use with either O_2 or H_2O as the oxygen source powered by electrons or light to perform sustainable OAT.

2. Electrochemical OAT

Electrochemical methods constitute an efficient way to bypass the use of chemical reagents. Taking inspiration from dioxygenase for oxygen activation and OEC for water oxidation, researchers are developing electrochemical procedures to fuel molecular catalysts using O_2 or H_2O as an oxygen source for

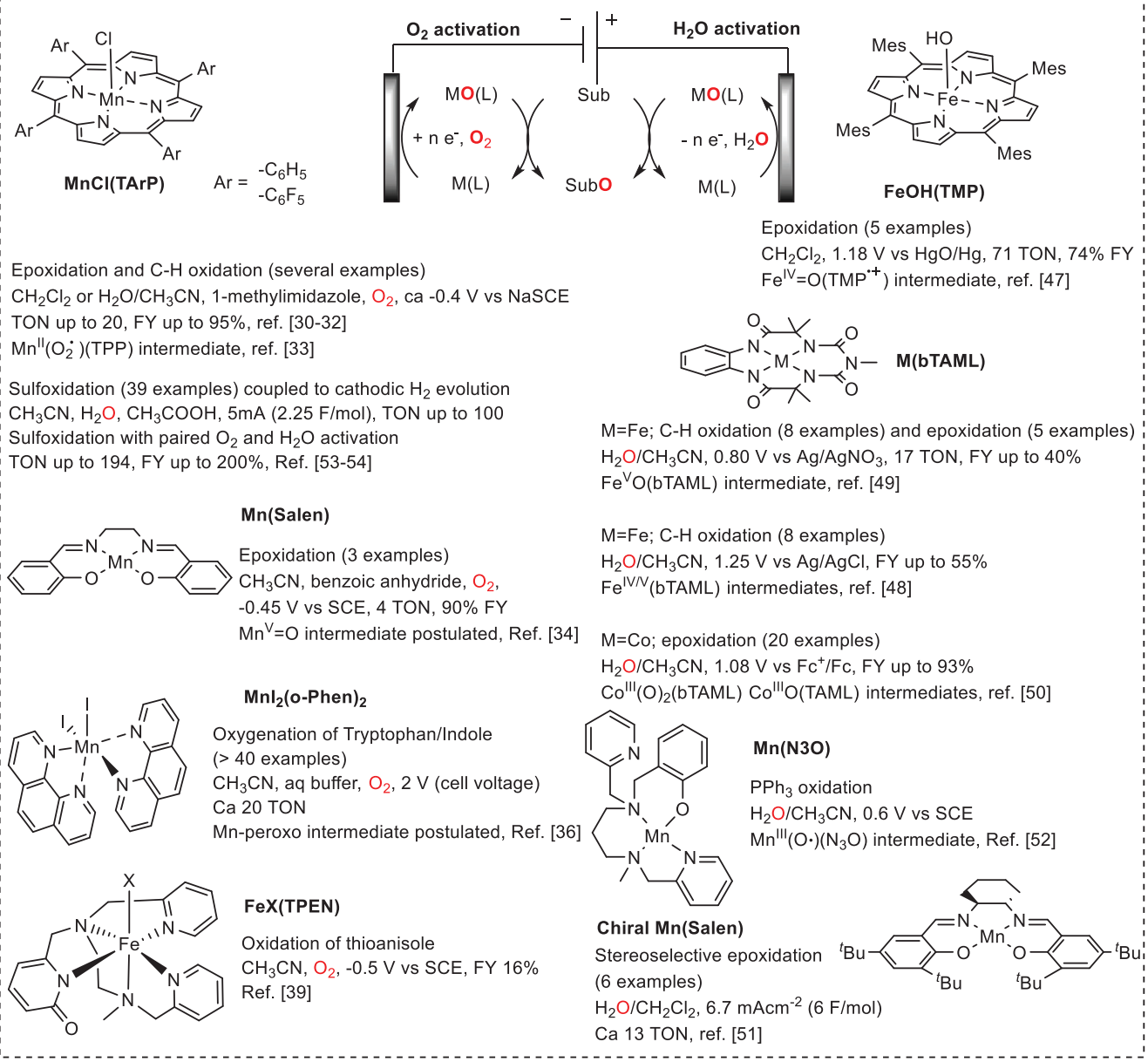

Scheme 2. Electrochemical routes toward OAT via O_2 or H_2O activation, and schematic representation of bioinspired metal catalysts employed, focusing on the OAT process and on the involved reactive intermediates.

OAT reactions (Scheme 2). The following paragraph outlines recent advancements in this field, with a focus on complexes of first-row transition metals.

2.1. Electrochemical Reductive Activation of O_2

Bioinspired molecular catalysts have emerged as transformative solutions for electro-assisted oxidation reactions, particularly through the electrochemical reduction of O_2. Taking clues from natural enzymes, molecular electrocatalysis aims to overcome the inefficiencies of conventional methods by providing sustainable alternatives for energy conversion technologies. This electrochemical approach avoids harsh reagents, aligning with green chemistry principles. Today, only a few cases of metal-based molecular complexes have been implemented for electrochemical O_2 activation. Such molecular catalysts mainly involve Mn and Fe complexes. Few examples have been reported with other metals, including Ru-salen [27] and Cu-azomethine.[28] A recent example using Cu describes the electrocatalysis of selective methane oxidation with O_2 by immobilizing tricopper catalysts on the cathode surface of an electrochemical cell.[29]

Murray and Mansuy's contributions pioneered electrochemical oxidations through the reductive activation of O_2 with metal tetraarylporphyrins (TArP).[30–32] Murray reported that $Mn^{III}Cl$(TPP) (TPP = tetraphenylporphyrin) could achieve epoxidation under reductive electrocatalytic

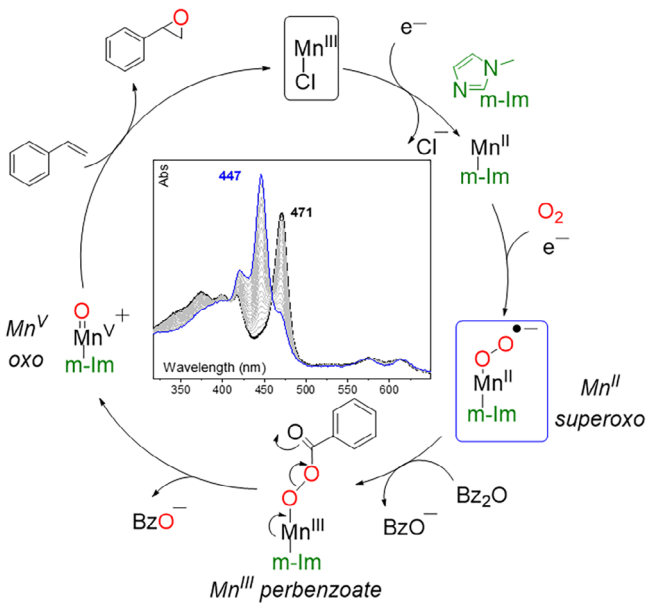

Figure 1. Mechanism of electrochemical epoxidation with $Mn^{III}Cl(TPP)$ with 1-methylimidazole (m-Im) and benzoic anhydride (Bz_2O) additives, with spectroelectrochemical evidence of Mn^{II} superoxo intermediate. Adapted with permission from Ref. [33].

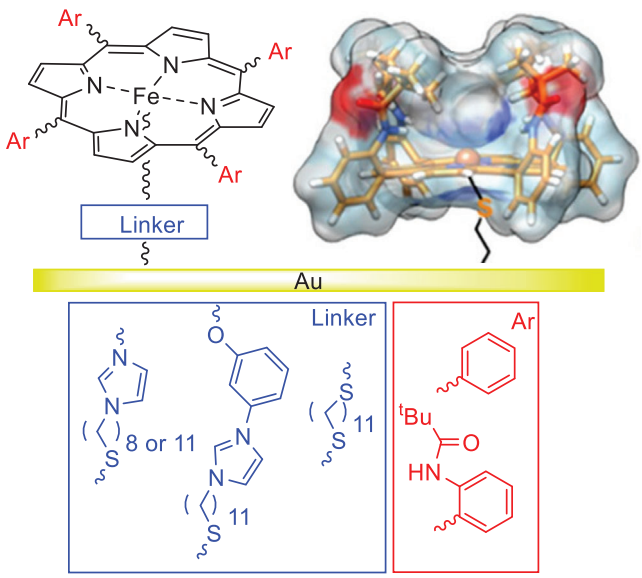

Figure 2. Heterogenization of iron porphyrins onto gold electrodes proposed by Dey and co-workers. Adapted with permission from Refs. [41–43].

conditions in the presence of 1-methylimidazole and benzoic anhydride. He highlighted the role of 1-methylimidazole coordinating to manganese as an axial ligand and proposed a mechanism involving the electrochemical reduction of Mn^{III} to Mn^{II} that can bind dioxygen and undergo a further reduction to form a $Mn^{II}O_2^{\cdot-}$ superoxo species. This intermediate undergoes the cleavage of the O—O bond assisted by benzoic anhydride to give the high-valent Mn^{V}=O, being the active species for epoxidation of styrene (Figure 1). More recently, some of us definitively proved that Mn^{II} superoxo participates in this process using spectroelectrochemistry.[33] Additionally, it was shown that the axial ligand significantly influences reactivity, as evidenced by the halogenation of cyclooctene when 1-methylimidazole is replaced with chloride.

Murray[34] and Moutet[35] observed similar results using an Mn(Salen) catalyst, although the stability of the active species was lower. Recently, Weng introduced an MnI_2(o-phen)$_2$ catalyst (o-phen = 1,10-phenantroline)[36] undergoing a bioinspired hydroperoxo key intermediate in the aerobic electrochemical oxygenation of tryptophan indole derivatives, demonstrating remarkable tolerance toward various functional groups. Notably, this reactivity has been successfully transferred from homogeneous solution to heterogeneous surface. Guo and Wong[37] showed that electropolymerized chiral manganese Schiff-base complexes can serve as catalysts for epoxidation of alkenes. They highlighted the significant impact of incorporating reactive metal species into the polymer network on both oxidation efficiency and TONs. Simultaneously, Simonneaux suggested employing porous electrodes as supports for Murray's conditions, enhancing the stability of the catalytic system and facilitating product separation post-electrolysis.[38]

Non-porphyrin Fe^{II} complexes are notable for their ability to generate reactive intermediates similar to those found in enzymatic cycles. In particular, Banse's group reported an iron TPEN (TPEN = *N,N,N′,N′*-tetrakis(2-pyridinylmethyl)-1,2-ethanediamine) complex that can reductively activate O_2 allowing the oxidation of thioanisole.[39] Recently, it has been demonstrated that second-sphere interactions, especially hydrogen-bonding, significantly improve O_2 activation and enhance substrate selectivity.[40] Another attractive approach involves anchoring the complex onto an electrode surface, thereby generating the intermediate species directly on the electrode rather than in solution. In this respect, Dey and Mukherjee have reported numerous examples of thiolate-bound Fe porphyrin immobilized on electrodes via self-assembled monolayer, designed to mimic the cytochrome P450 active site (Figure 2).[41] By introducing an axial thiolate ligand, they have leveraged the synergistic push effect that promotes cleavage of the O—O bond and extends the lifetime of the oxidizing species. Additionally, they minimized direct O_2 reduction at the electrode by anchoring the reactive species to the surface. Under these conditions, they reported catalytic hydroxylation of alkanes to alcohols and epoxidation of alkenes by Fe^{IV}=O,[41] as well as the oxidation of 2,3-dimethyl indole via Fe^{III}-superoxo intermediates, with $>6{\cdot}10^4$ turnovers.[42,43]

2.2. Electrochemical Oxidative Activation of H_2O

High-valent metal-oxo species may also be accessed electrochemically through proton-coupled oxidation of metal-aquo species. This approach has been extensively explored, particularly in the context of four-electron water oxidation leading to the oxygen evolution.[44,45] Surprisingly, however, oxygenation of organic substrates via electrochemically generated metal-oxo species has received relatively little attention. Early work by Khan in 1989[46] reported the formation

Minireview
DOI:10.1002/anov.70007

GDCh German Chemical Society

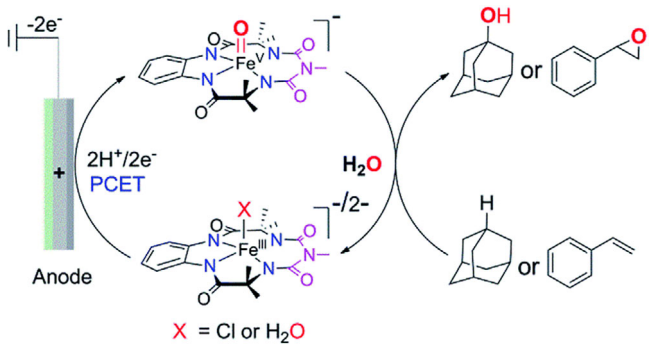

Figure 3. Electrochemical approach to forming the $Fe^{V}O$(bTAML) complex from the initial $Fe^{III}X$(bTAML) complex (X = H_2O or Cl^-). Reprinted with permission from Ref. [49].

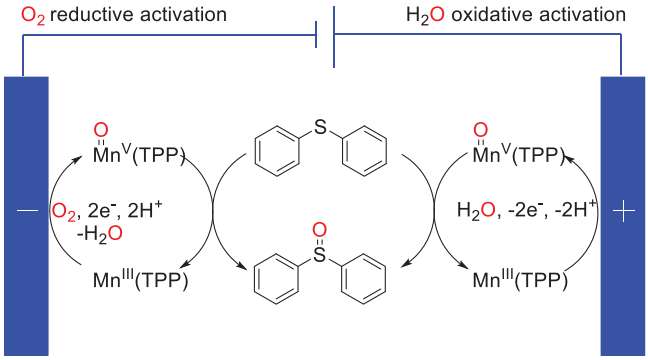

Figure 4. Scheme of paired electrolysis test for Ph_2S oxidation reported by Stahl, adapted from Ref. [54].

of high-valent $Ru^{VI/VII}$-oxo intermediates supported by a dimethylglyoxime (dmg) ligand resulting from electrochemical oxidation of Ru^{III}(H-dmg) in an aqueous medium. Other seminal papers include Groves's work on Fe porphyrin complexes,[47] which demonstrated the electrochemical generation of Fe^{III}—OH and Fe^{IV}=O species. Notably, Groves achieved the electrocatalytic epoxidation of olefins using an Fe(TMP) catalyst (TMP = tetramesitylporphyrin) without the need for oxygen-donating oxidants. More recently, iron oxo species with biuret-modified tetraamido macrocyclic ligand (bTAML) have been obtained via electrochemical proton-coupled oxidation of the corresponding Fe^{III}—OH_2(bTAML) complexes. Fe^{IV} and Fe^{V} species were evidenced and led to the electrochemical oxygenation of benzylic C—H bonds and dehydrogenation of alcohols to ketones.[48] Shortly after, Chandra et al. reported a selective electrochemical oxygenation of unactivated C—H and C=C bonds mediated by Fe(bTAML) and using water as the oxygen source.[49] Mechanistic studies point to the involvement of a high-valent $Fe^{V}O$(bTAML) species in these transformations, Figure 3.

Very recently bTAML ligand were also exploited to form Co complexes for olefin substrate epoxidation in the presence of water. Operando voltammetry-electrospray ionization mass spectrometry and electron paramagnetic resonance analyses were utilized to probe cobalt oxygen active intermediates. The mechanism involved a rate-limiting proton-coupled electron transfer process, forming reactive cobalt oxygen active species from the $2e^-$ oxidized $[Co^{III}(bTAML)]^-$.[50]

The electrochemical approach was also expanded to perform stereoselective OAT. Using chiral manganese Schiff-base complexes introduced by Wong and Guo for reductive O_2 activation,[37] Tanaka and co-workers reported the asymmetric electrochemical epoxidation of olefins in a CH_2Cl_2/H_2O two-phase system. The proposed mechanism involves highly oxidant Mn-oxo species, formed upon reaction of the Mn^{III}(Salen) complex with ClO^- generated from the electro-oxidation of Cl^- in the aqueous phase.[51] Later, taking inspiration from the oxygen-evolving complex in Photosystem II, Lassalle Kaiser et al. attempted to electrogenerate high valent Mn-oxo species from a mononuclear $Mn^{II}(N_3O)$ complex. Reactivity patterns (very low OAT and HAT abilities), DFT calculations, and XANES pre-edge features provided strong evidence that the bonding oxo species was best described as an Mn^{III}-oxyl species.[52]

More recently, the group of Stahl showed that Mn porphyrins can be effective electrocatalysts for selective oxidation of thioethers to sulfoxides at modest electrode potentials in excellent yields. The electrochemical reaction proceeded via a proton-coupled oxidation of a Mn^{III}—OH_2 species to generate a Mn^{IV}—OH and Mn^{V}=O species.[53] The same group also reported an elegant process combining simultaneous O_2 and H_2O electrochemical activation, reproducing monooxygenase activity at the cathode and dehydrogenase activity at the anode. Using Mn^{III}(TPP) as a catalyst for both reactions, they succeeded in generating a reactive Mn^{V}=O(TPP) at both electrodes. This tandem system allowed the OAT reactivity to two thioether substrates, generating two equivalents of sulfoxide, with a ca 200% combined FY, accounting for both anodic and cathodic contributions (Figure 4). Although the net dioxygenase reactivity consumes no electrons, it still necessitates electrochemical energy to overcome kinetic barriers. The authors provided a thorough analysis of the electrochemical metrics, which will guide the development of (electro)catalysts for chemical synthesis, demonstrating dioxygenase reactivity.[54]

3. Photochemical OAT

Chemists are dedicating considerable efforts to harnessing photons as the sole energy input to drive OAT. This strategy exploits light as a physical reagent to promote electron transfer chains to a metal catalyst, enabling either O_2 or H_2O activation.[55,56] This is achieved classically by exposing to irradiation a multicomponent system, comprising a photosensitizer, the metal catalyst, and either a sacrificial electron donor (SED) for the reductive activation of O_2, or a sacrificial electron acceptor (SEA) for the activation of H_2O (Scheme 3). However, the photochemical approaches face additional difficulties given the unavoidable occurrence of parasitic processes, including unproductive back electron transfer and undesired quenching (especially when O_2 is present).

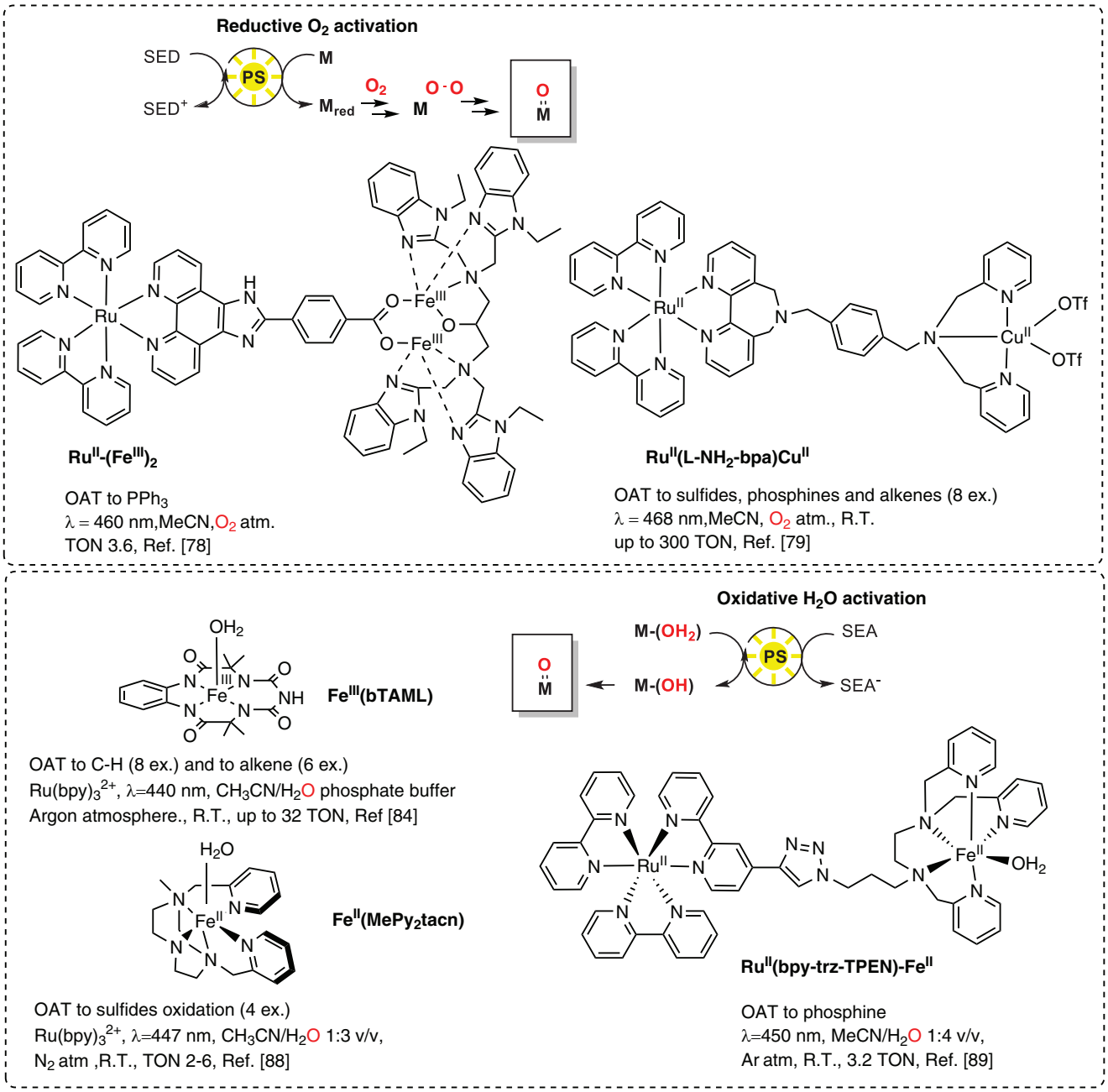

Scheme 3. General principles for O_2 or H_2O photochemical activation, and selected examples of molecular systems combining transition metal complexes with photosensitizers. More examples can be found in the literature.[57–60]

3.1. Photochemical Activation of O_2

Seminal studies have focused on the photochemical generation of metal-oxo species via direct excitation of the parent metal complex.[61–65] Activation of O_2 was achieved through a strategy adopted by Nocera and coworkers that reported OAT to phosphines, sulfides, olefins and hydrocarbons with a di-iron(III) μ-oxo porphyrin photocatalyst, where the two co-facial porphyrin moieties are linked by a spacer (Figure 5).[66,67] The iron(IV) species responsible for OAT reactivity was generated by disproportionation induced by UV-irradiation of the μ-oxo dimer, which was restored through reactivity with O_2 as the oxygen source. A proper length of the covalent spacer modulates the pocket dimension for hosting the substrate while preventing the recombination to the former μ-oxo diiron(III) states. A similar strategy was pursued by Harischandra and co-workers with a bis-corrole-diiron(IV) dimer.[68]

This approach presents some limits due to significant recombination, which limits the productive oxidative pathways and the quantum yield. These restraints prompted the investigation of dyadic systems, where the light harvesting/charge separation and OAT functionalities are provided by different moieties.

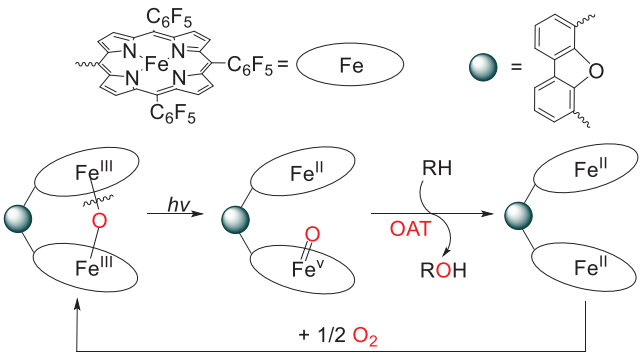

Figure 5. Photochemical OAT with a di-iron(III) μ-oxo porphyrin photocatalyst, where the two co-facial porphyrin moieties are linked by a spacer.[66,67]

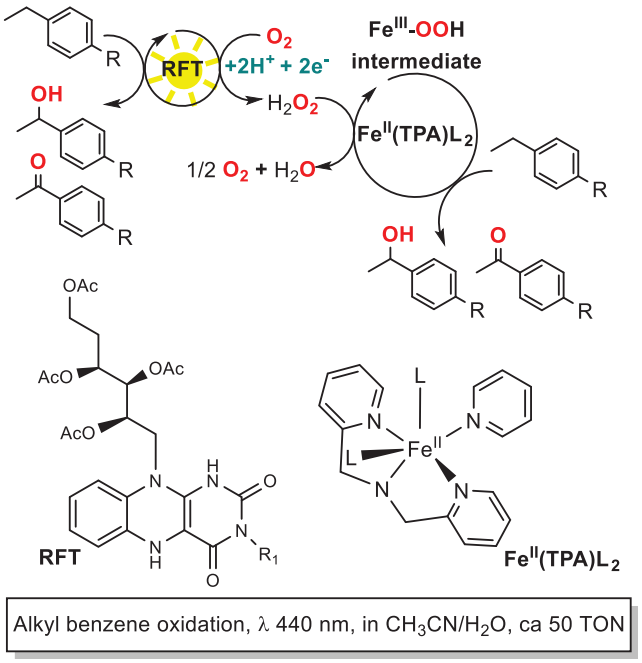

Figure 6. Dual photocatalysis for the oxygenation of alkyl arenes, combining RFT for the photochemical production of H_2O_2 and the $Fe^{II}(TPA)L_2$ catalyst; L stands for an apical ligand, typically acetonitrile solvent.[76]

Flavins models inspired from flavoenzymes were long investigated for their photocatalytic properties.[69–71] König and colleagues reported photocatalytic OAT of ethylbenzenes to the corresponding ketones using Riboflavin Tetraacetate (RFT) and electron donors, where O_2 is photochemically reduced to form H_2O_2, that however lead to degradation of RFT.[72,73]

Wolf and collaborators cleverly capitalized in exploiting H_2O_2 in a dual catalytic system that combined both RFT and a non-heme $Fe^{II}(TPA)L_2$ complex (TPA = tris(2-pyridylmethyl)amine; L = apical ligand),[74,75] (Figure 6).

The iron complex reacted with the generated H_2O_2 to form the active iron(III)-hydroperoxo species, which participated in the oxygenation of alkylbenzenes.[76] This combined catalysis approach provided the benefits of accelerating the oxidation cycle while protecting the RFT from deleterious bleaching with H_2O_2.[74,75,77]

The photoactive component can also mediate the transfer of reducing equivalents to the metal complex, enabling its interaction with O_2. H. Gray and coworkers have pioneered this field by activating a member of the cytochrome P450 family of enzymes using a covalently tethered ruthenium(II) tris(bipyridine) photosensitizer. Unlike the classic pathway involving reductive activation of O_2, their approach enables the photocatalytic oxidative activation of water at the heme site, leading to the formation of highly oxidized species capable of performing OAT.[78] An early example involving synthetic catalysts dealt with a ruthenium(II) polypyridine sensitizer with an appended carboxylate pendant to bind a dinuclear iron(III) complex as a model of methane monooxygenase (Ru^{II}–$(Fe^{III})_2$ in Scheme 3).[77] Under irradiation in presence of triethylamine, the authors observed the formation of the putative bis Fe^{IV}=O dimer from a two-electron reduction of the parent diiron core followed by binding of O_2. Photochemical OAT to triphenyl phosphine was observed, although it was evidenced that the separated components functioned better than the supramolecular assembly. This adverse effect highlights a crucial issue when designing molecular dyads, i.e., the occurrence of back electron transfer events; nevertheless, the dyadic design inspired other photochemical systems for O_2 activation.

Hamelin and colleagues reported a molecular dyad system composed of ruthenium(II) photosensitizer and copper(II) catalyst (Ru^{II}(L-NH_2-bpa)Cu^{II}, Scheme 3) that could promote OAT to sulfides, triphenylphosphine, indene and cycloalkenes, under visible light irradiation in the presence of triethanolamine (up to 300 TON).[79] The photoreduced copper(I) species was monitored using EPR spectroscopy, and its observed reactivity in the presence of O_2 was attributed to the formation of a Cu^{II}–O_2^- (copper(II) superoxo) species, responsible for OAT. Similar Ru^{II}–Cu^{II} covalent dyads were proposed for aerobic OAT to sulfides by Chao and Zhao[58] and by Klein et al.[59]

A reversible electron relay was incorporated into a traditional intermolecular photosensitizer/catalyst system, eliminating the requirement for a SED.[80] The system comprised a $[Ru^{II}(bpy)_3]^{2+}$ photosensitizer, an Fe^{III}(DPPy) catalyst (DPPy = DipyrrinDiPyridine), and a methyl viologen (MV^{2+}) mediator (Figure 7). An efficient oxidative quenching of $*[Ru^{II}(bpy)_3]^{2+}$ by MV^{2+} produces the methyl viologen radical ($MV^{\bullet+}$) and $[Ru^{III}(bpy)_3]^{3+}$. $MV^{\bullet+}$ acts as a reducing agent of both O_2 and Fe^{III}(DPPy), forming the superoxide radical anion $O_2^{\bullet-}$ and Fe^{II}(DPPy) that combine to form Fe^{III}-hydroperoxo (Fe^{III}–OOH) intermediates. These can subsequently evolve into a highly oxidized iron-oxo species, enabling the OAT to sulfonate styrene derivatives in water, producing epoxides or diols.

A similar scheme was proposed also for OAT to alkenes, employing an air stable, non-heme Fe^{II}(L5) catalyst, where L5 = *N,N′,N′*-tris(2-pyridylmethyl)ethane-1,2-diamine (Figure 7).[81] These studies indicate that incorporating a reversible single-electron mediator provides a solution to the challenging issue of charge buildup at the molecular catalytic site during the two-electron activation of O_2.

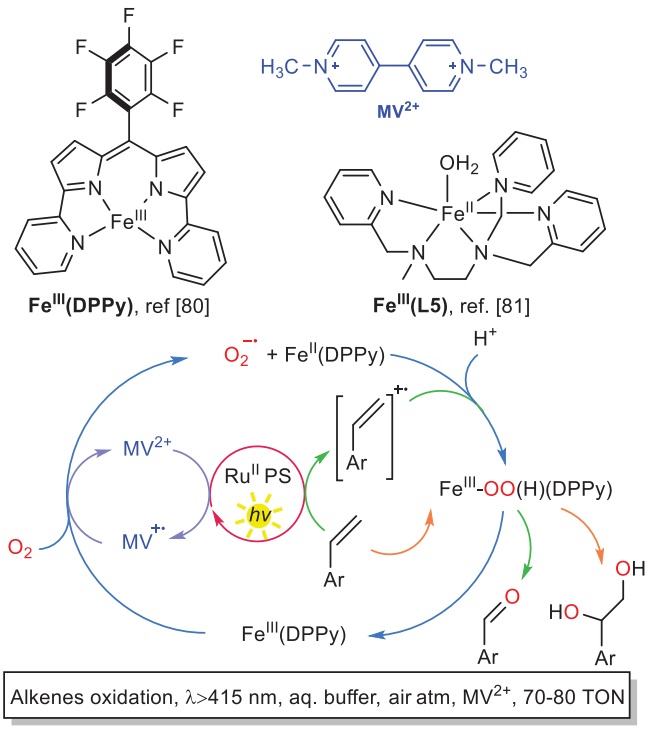

Figure 7. OAT photocatalysis with O_2 activation in the presence of MV^{2+} redox mediator.[80,81]

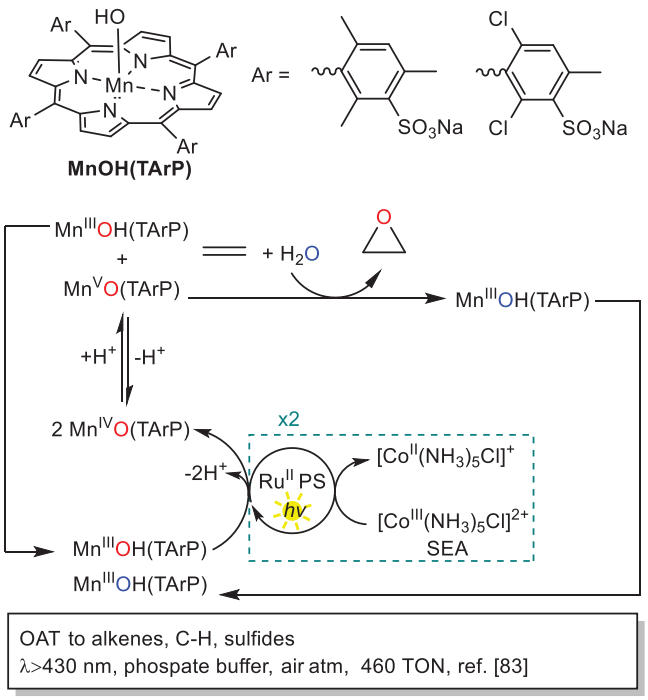

Figure 8. Photocatalytic oxidation of alkenes to epoxides with H_2O as oxygen source with $[Ru^{II}(bpy)_3]^{2+}$, Mn^{III} porphyrin catalysts, and $[Co^{III}(NH_3)_5Cl]^{2+}$ SEA.[83]

3.2. Photochemical Activation of H_2O

Calvin and colleagues reported the photoactivation of a manganese porphyrin in the presence of $[Ru(bpy)_3]^{2+}$ and of a cobalt(III) salt as SEA, observing the formation of a high-valent metal-oxo species under irradiation.[82] Building on this concept, Nam and collaborators reported the photocatalytic conversion of styrene sulfonates to the corresponding epoxides using water as the oxygen source (Figure 8).[83]

Upon light absorption, $*[Ru^{II}(bpy)_3]^{2+}$ undergoes oxidative quenching with the Co^{III} acceptor, and the $[Ru^{III}(bpy)_3]^{3+}$ oxidizes the Mn^{III} porphyrin, converting it into $Mn^{IV}O(TArP)$ (Figure 8). At this stage the $Mn^{IV}O(TArP)$ complex undergoes disproportionation to form the $[Mn^{V}O(TArP)]^{+}$ as OAT species while regenerating $Mn^{III}OH(TArP)$. This crucial disproportionation step avoids the need of a two-step charge accumulation starting from the $Mn^{III}OH(TArP)$.

Chandra and colleagues[84] have also observed a disproportionation step in photocatalytic OAT for epoxidation of alkenes and hydroxylation of alkanes mediated by a Fe^{III}(bTAML) catalyst,[22,85,86] Scheme 3. It is worth noting that this catalytic system represents the first example of alkane hydroxylation, emphasizing the high reactivity of the Fe^{V}=O(bTAML) species.[84]

Other examples[55] of non-heme complexes were reported by Fukuzumi and colleagues, with the photogeneration of an iron(IV)oxo from a $[Fe^{II}(OH_2)(N_4Py)]^{2+}$ complex ([N_4Py = *N,N*-bis(2-pyridylmethyl)-*N*-bis(2-pyridyl)methylamine].[87] Company and colleagues started from an Fe^{II}(MePy2tacn) (MePy2tacn = *N*-methyl-*N,N*-bis(2-picolyl)-1,4,7-triazacyclononane) in the presence of $[Ru^{II}(bpy)_3]^{2+}$ and persulfate ($S_2O_8^{2-}$) as SEA to photogenerate the corresponding $Fe^{IV}O$(MePy2tacn),[88] for OAT to sulfides as substrates. Of note, in most cases with non-heme complexes, OAT was reported with substrates containing heteroatoms (S and P mainly).

In general, the intermolecular approach requires a large excess of the photosensitizer and SEA to promote the light-induced multiple charge accumulation at the catalyst. To address this challenge, chemists have developed covalently linked photosensitizer-catalyst systems to facilitate intramolecular electron transfer, which is expected to be faster than the intermolecular process (Scheme 3).[60,89].

Another innovative design considered the simultaneous O_2/water activation for OAT to benzene with a $[Co^{III}(Cp^*)(bpy)(H_2O)]^{2+}$ catalyst (Cp^* = η^5-pentamethylcyclopentadienyl and bpy = 2,2'-bipyridine) and a Ru^{II} photosensitizer; the cobalt catalyst enabled both water oxidation to O_2 and activation of photochemically generated H_2O_2 for benzene hydroxylation, enabling ca. 500 TON.[90]

3.3. Photoactive Materials

Bioinspired strategies may also guide the development of catalytic materials. A recent example deals with photooxidation of methane to methanol via O_2 activation with a metal-organic framework (MOF) inspired by methane monooxygenase (Figure 9). The MOF integrated a $Ru^{II}(bpy)_2$(bpydc) photosensitizer, (bpy: 2,2′-bipyridine; bpydc: 2,2′-bipyridine-5,5′-dicarboxylate), a $[PW_9V_3O_{40}]^{6-}$ polyoxometalate for O_2

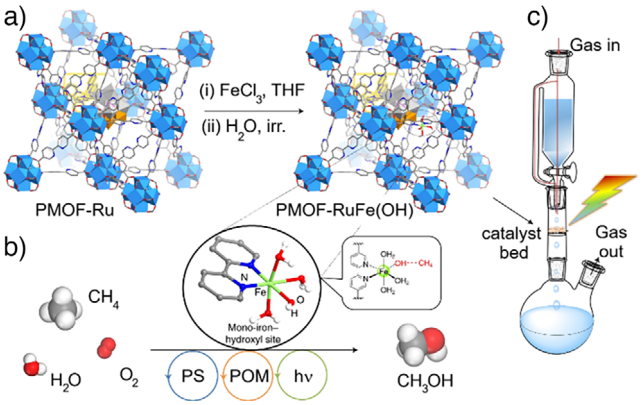

Figure 9. Photocatalytic metal-organic framework (PMOF-RuFe(OH)) for selective conversion of methane to methanol; a): representation of the material, b): photocatalytic scheme, c): implementation in a continuous flow apparatus. Reprinted with permission from Ref. [91].

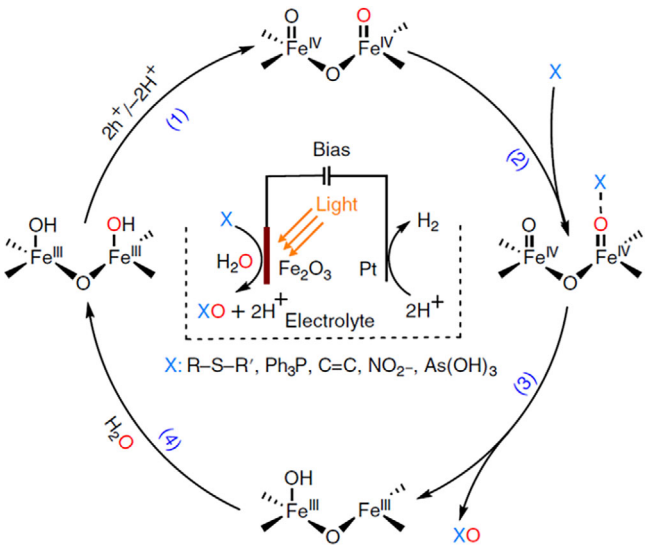

Figure 10. Photoelectrochemical generation of Fe^{IV}=O sites on the hematite surface and OAT to substrate X. Reprinted with permission from Ref. [103].

activation, and a mono-iron hydroxyl site to activate CH_4.[91] Methanol productivity reached 8.81 ± 0.34 $mmol g_{cat}^{-1} h^{-1}$ under ambient and flow conditions (5.05 $mmol g_{cat}^{-1} h^{-1}$ for methane monooxygenase), while a quantitative selectivity for methanol was achieved. This is in part explained by the postulated mechanism, where methanol is formed by coupling of ·OH and $\cdot CH_3$ radicals. Photoreduction of the POM by the excited Ru sensitizer drives the POM-assisted reduction of O_2 to H_2O_2, forming in situ ·OH radicals at the Fe—OH moiety under irradiation. In parallel, $\cdot CH_3$ radical formation occurs upon absorption of methane to the Fe—OH site. A kinetic H/D isotopic effect of 3.0 ± 0.4 between CH_4/CD_4 indicates the C—H activation as the most likely rate-determining step.

We also mention an example of OAT promoted by a Mo-based MOF photocatalyst. Molybdenum is a transition metal found in biological systems; recently, a *cis*-$Mo^{VI}O_2$ complex was reported to induce photoinduced OAT between phospines and sulfoxides, although it was unable to activate water and dioxygen.[92] Instead, Van Der Voort and co-workers reported a dioxo-molydbenum(VI) based MOF able to promote the photo-epoxidation of (α,β)-pinene through selective OAT via activation of O_2 proceeding through Mo^{VI} peroxo intermediates (99% selectivity toward α-pinene oxide with blue light, with recyclability of the catalyst).[93] The field is in rapid expansion and also includes the use of covalent organic frameworks (COFs). Photoactive COFs based on thienothiophene chromophores were recently exploited for the epoxidation of styrene derivatives, although the system required the presence of bicarbonate for the activation of water through the formation of a peroxycarbonate OAT agent.[94]

The photochemical reactivity of iron-based materials toward OAT was also investigated considering hematite (α-Fe_2O_3) photoanodes. Hematite was indeed long investigated as an active n-type semiconductor for water splitting applications;[95–97] more recently, n-type semiconductors (eventually dye-sensitized) have been considered also for oxidative organic synthesis.[98–102] Zhao and co-workers targeted the application of hematite materials toward OAT to a variety of substrates, with water being the source of oxygen (Figure 10).[103] The system works through surface generation of Fe^{IV}=O sites after trapping the photoexcited holes, while electrons are conveyed to the counter electrode. The authors proposed the necessity of generating two adjacent Fe^{IV}=O sites, with rate-determining "two-electron" OAT to the substrate from one Fe^{IV}=O moiety, concomitant to electron transfer to the neighboring Fe site to restore a {Fe^{III},Fe^{III}} state, followed by water binding.

Concerning performance metrics, at a mild potential of 0.37 V vs. Fc^+/Fc, the α-Fe_2O_3 photoelectrode provides ca. 0.3 mA cm^{-2} photocurrent density for the photoelectrochemical OAT to methyl phenyl sulfide, achieving >85% conversion with an almost quantitative selectivity for the sulfoxide and >90% FY. A maximum 22% incident photon to current efficiency (IPCE) was obtained at 330 nm, while the system can operate up to 550 nm. The authors highlighted the pros of the hematite material on the selectivity of the OAT, in comparison with other semiconductors, and postulated this result was a consequence of the active species involved in the mechanism.

The development of photoactive materials has recently followed alternative pathways, taking advantage of sustainable biomaterials coupled with enzymes.[104] This approach enabled the stereoselective oxygenation of unactivated C—H bonds by activating a peroxygenase biocatalyst (>45 000 turnovers) through the use of photoactive artificial wood consisting of lignin arranged around cellulose fibers.[105] A significant amount of new contributions is expected to emerge in this field.

4. Organic Photocatalysis and Electrophotocatalysis

Examples of photochemical OAT are not limited to the use of transition metal complexes. Light enables the activation of organic photocatalysts operating through non-conventional

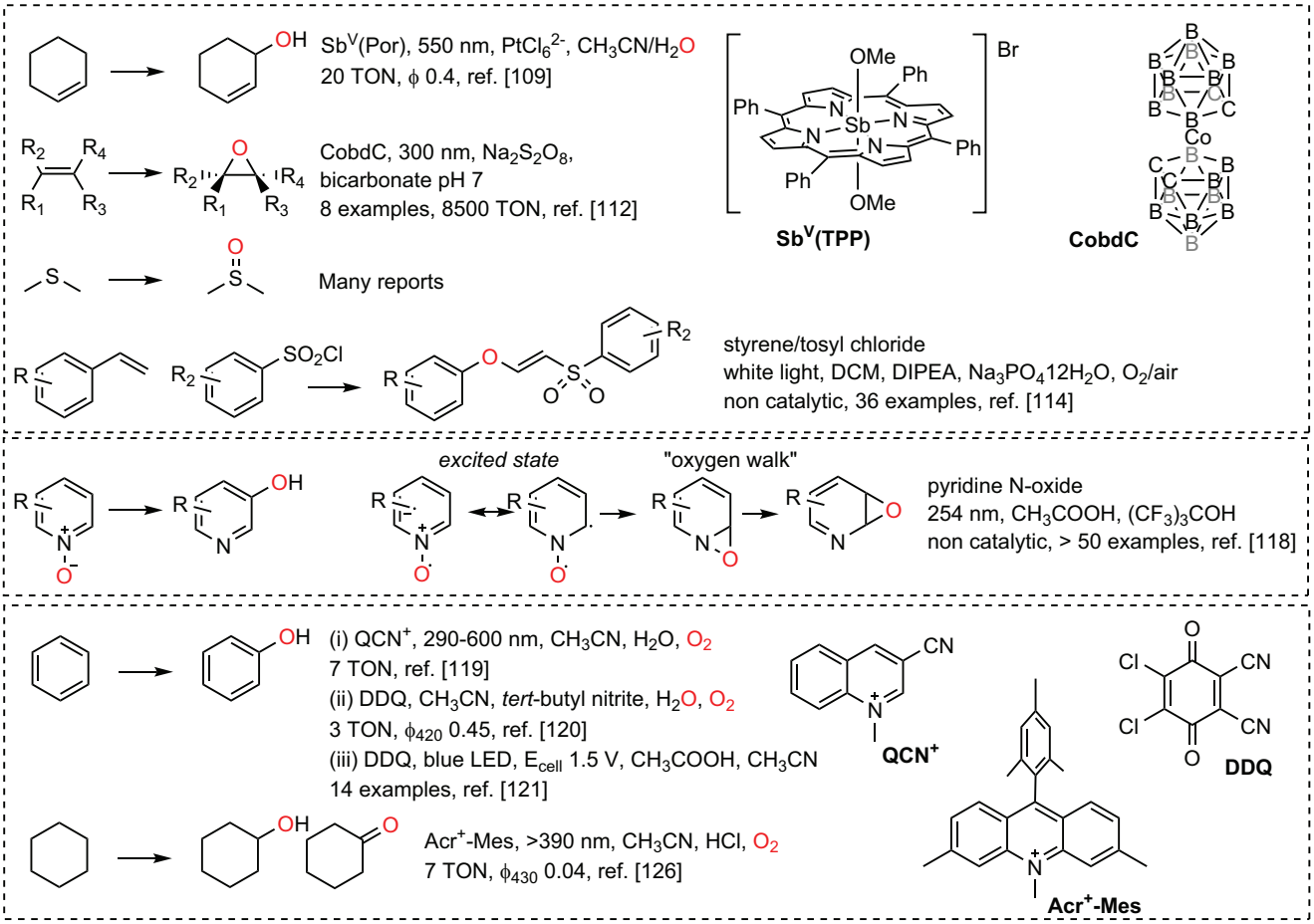

Scheme 4. Selected examples of OAT with organic photocatalysts.

routes, possibly in combination with electrochemical activation. Nevertheless, examples of selective, photochemical OAT through O_2 and water activation exploiting organic photocatalysts are limited[106] and follow peculiar mechanisms (Scheme 4).[107,108] A Sb^V(TPP), characterized by a highly oxidizing excited state, was capable of photooxidation via single electron transfer (SET) of cyclohexene, followed by allylic hydroxylation in the presence of water.[109] A similar system was reported with Al^{III} porphyrinoids[110,111] and for a cobalt bis(dicarbollide) photoredox catalyst for the epoxidation of alkenes in water.[112] Several organic photocatalysts have been employed for the OAT to sulfides.[113] A non-catalytic example of oxygenation of organic compounds deals with the aerobic photochemical transformation of styrene into aryl ether frameworks (Scheme 4).[114] In this paragraph we will report selected examples of organic photocatalysis for OAT involving challenging C─H bonds.

In 1970, Boyd and co-workers observed the photochemical OAT from pyridine N-oxide to naphthalene with the formation of 1,2-naphtalene oxide and 1-naphtol.[115–117] A recent example exploited these findings, developing the hydroxylation of pyridines at the C3 position via UV activation of pyridine N-oxide (π–π^* transition) in the presence of acetic acid and $(CF_3)_3COH$ additives (Scheme 4).[118] ^{18}O labeling studies demonstrated the preservation of the isotopic label in the 3-pyridinol product, suggesting an intramolecular "oxygen atom walk" pathway. Although the system is not catalytic, it provides an interesting example of photochemical OAT in challenging aromatic hydroxylation for organic synthesis. Indeed, the photocatalytic hydroxylation of aryl C─H bonds was initially explored with potent photooxidants, with one of the fist examples taking advantage of a quinolinium ion photocatalyst (QCN^+), enabling conversion of benzene to phenol with concomitant formation of H_2O_2 (Scheme 4).[119] A breakthrough was reported by Ohkubo et al. upon demonstrating hydroxylation of benzene with visible light activation of 2,3-dichloro-5,6-dicyano-*p*-benzoquinone (DDQ), in the presence of water as the oxygen atom source.[120] Transient absorption experiments suggested oxidation of benzene via SET by the ^{3}*DDQ excited state (E = 3.18 V vs. SCE for the ^{3}*DDQ/DDQ$^{\bullet-}$ couple). The possibility of operating catalytically (3 TON in 30 h) was achieved by introducing *tert*-butyl nitrite redox mediator to assist aerobic reoxidation of reduced DDQ. The DDQ photochemical reactivity was implemented in an electrochemical cell by Lambert and Huang, where re-oxidation of reduced DDQ was conducted at a carbon anode, coupled to cathodic hydrogen evolution.[121] An in-flow setup enabled the achievement of conversion of benzene to phenol on a gram scale, although it still necessitated a high 10% DDQ amount due to limited TONs also in the

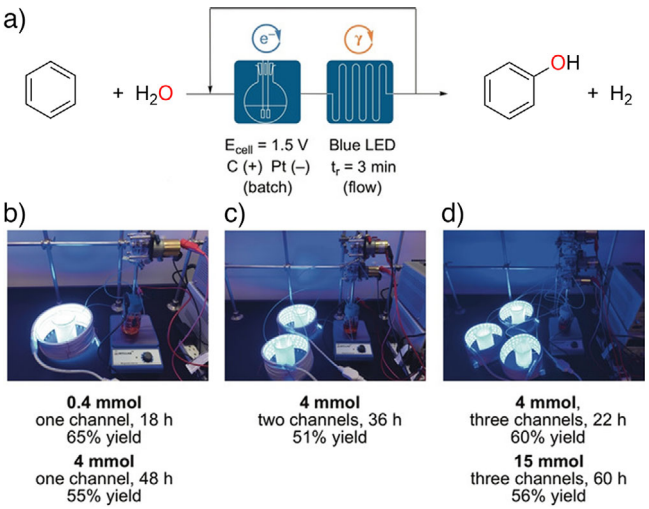

Figure 11. a) In-flow photo-electrochemical system for benzene hydroxylation to phenol catalyzed by DDQ. b)–d) Pictures of the flow photoreactors. Reprinted with permission from Ref. [121].

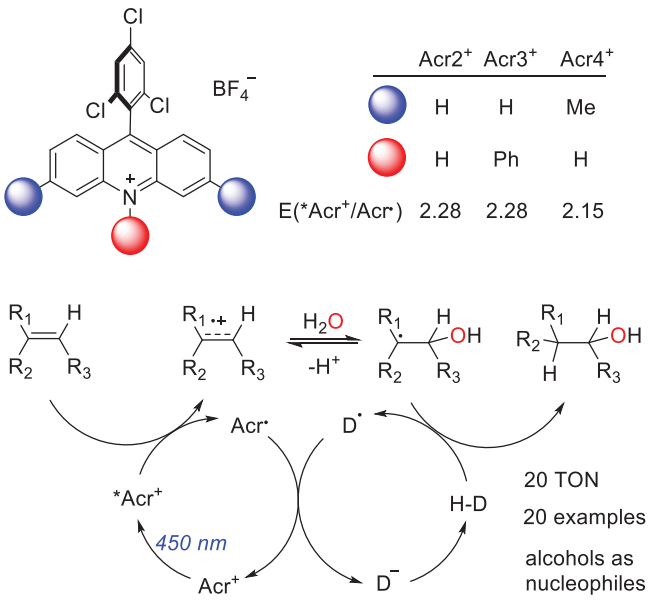

Figure 12. Photocatalyzed anti-Markovnikov hydration of olefins by highly oxidizing acridinium photocatalysts with 2,4,6-trichlorophenyl substituent at the 9-position.[128]

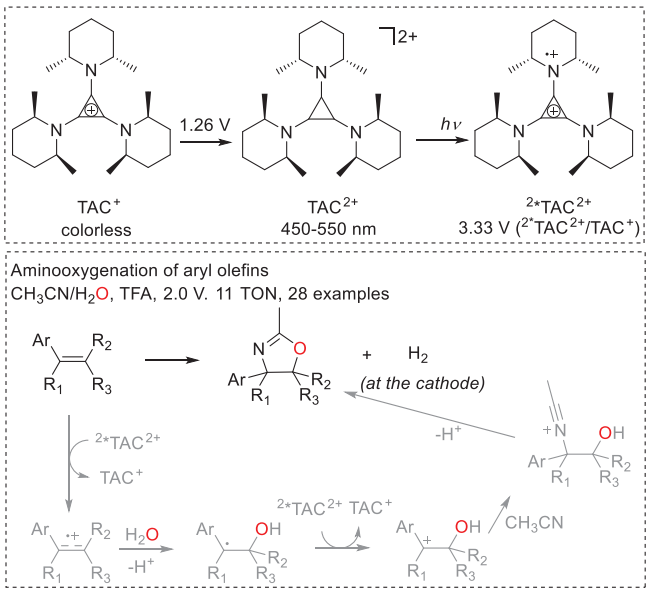

Figure 13. Representation of TAC^+ derivatives, and electrophotochemical aminooxygenation of aryl olefins where water is trapped by the radical cation of the aryl olefin substrate.[137]

electrophotocatalytic conditions (Figure 11). DDQ was also used for aryl C–H transformation to ethers/esters/anilines by adding alcohols/acids/amines as coupling agents.[122] These works unleashed the potential of quinone triplet excited states as powerful oxidants, enabling both SET and hydrogen atom abstraction.[123–125]

Another class of extensively investigated photooxidants is acridinium ions. The field was pioneered by Fukuzumi and coworkers, reporting cyclohexane aerobic oxidation to KA oil by 9-mesityl-10-methylacridinium ions (Acr^+–Mes) with visible light. A radical autooxidation was postulated, starting from the generation of Cl· radicals from Cl^- oxidation by the excited Acr^+–Mes.[126] The photoactivity of acridinium ions was further exploited for benzylic oxygenation of alkyl arenes to the corresponding carbonyl compounds.[127] A most interesting application dealing with OAT was recently reported by Worp et al.[128] The oxidizing power of the acridinium excited state was boosted by the installation of an electron-withdrawing 2,4,6-trichlorophenyl moiety at the 9-position, reaching up to 2.28 V vs. SCE. This was pivotal in enabling an oxidation via SET of olefin substrates, followed by hydroxylation of the olefin radical cation with water; a hydrogen atom donation closes the cycle to provide the hydroxylated product (Figure 12). The reaction shows enormous synthetic appeal since the reactivity can be extended by replacing water with other nucleophiles. Acridinium photocatalysts have been recently considered for oxidative upcycling of polystyrene by De Abreu et al., via generation of reactive oxygen species.[129] Acr^+–Mes was also exploited for carboxyhydroxylation and aminohydroxylation of α-olefins catalyzed by pyridine N-oxides and exploiting water as an oxygen source.[130]

The generation of potent photooxidants can follow alternative routes, including a combined electro- and photochemical activation.[131–133] One prominent example is the trisaminocyclopropenium ion (TAC^+) proposed by Lambert and co-workers (Figure 13).[134] One-electron electrochemical oxidation of colorless TAC^+ to TAC^{2+} (at mild 1.26 V vs. SCE) and visible light irradiation of TAC^{2+} (up to 550 nm) enables the generation of $*TAC^{2+}$ super-oxidant ($E \approx 3.33$ V vs. SCE). $*TAC^{2+}$ is indeed capable of SET from benzene to generate its radical cation (E = 2.48 V vs. SCE), further involved in oxidative couplings with azoles,[134] for acetoxyhydroxylation of aryl olefins,[135] for oxygenation of multiple adjacent C–H bonds,[136] and for aminooxygenation of aryl olefins to oxazoline scaffolds. We focus on this last example since it involves water as the primary OAT agent

to the substrate (Figure 13).[137] After oxidation of the aryl olefin by *TAC^{2+}, the olefin radical cation undergoes deprotonation and water trapping to form a hydroxylated benzyl radical intermediate that faces a second one-electron oxidation and ultimately entraps an acetonitrile molecule to give the oxazoline product after intramolecular cyclization.

5. Summary and Outlook

In this minireview, we have discussed OAT processes through electrochemical or photochemical activation of dioxygen and water. We started from seminal works reported in the field to discuss recent advancements. In this final section, we present challenges and possible future developments of OAT processes.

1. The design of functional components constitutes the primary brick for the realization of efficient catalytic routines: we believe that a molecular design will always retain a primary role. In the context of OAT, a specific target could be the development of bifunctional systems for simultaneous activation of both O_2 and H_2O, possibly employing the same catalyst. The use of bifunctional routines is currently an emerging approach also in the overall/hybrid water splitting context,[138] and should contribute to getting rid of sacrificial acceptors/donors to feed the complementary redox routes: the concept of "overall redox-neutral cycles" has emerged, where the two semi-reactions are both productive toward target transformations.[139] Related to light activation, the development of new cheap and accessible light-harvesting molecules and materials is highly desirable, in particular for targeting the low-energy region of the solar spectrum.[140] Other components that are often overlooked are redox mediators,[141–143] that should promote the desired transfer of electrons while hampering unproductive parasite processes.

2. While this minireview focused on bioinspired transition metal complexes and organic photocatalysts, other approaches have exploited different intermediates, including reactive oxygen species,[144] radicals, or other oxidants generated in situ. Recent examples have demonstrated the possibility of using simple mediators (Cl^-, Br^-, NO_3^-) under electrochemical[145,146] and photoelectrochemical[147–149] conditions, enabling OAT with high performance. These mediators also offer the possibility to guide the reaction mechanism. For example, Cl^- enables activation of water through formation of HOCl as an OAT agent for epoxidation reactions; electrochemical oxidation of NO_3^- produces $NO_3^{\bullet}$ as a hydrogen atom abstractor. Besides the efficiency of the processes developed so far in terms of yield, productivity rate, Faradaic or quantum yields, one further aspect to be addressed in electrochemical or photochemical OAT via these intermediates concerns selectivity control.

3. Real applications should preferably take advantage of heterogeneous rather than homogeneous systems. The heterogeneous engineering of functional molecular components is not a trivial step. The introduction of specific anchoring groups requires additional demanding synthetic steps, and the resilience of a covalent anchoring depends on the operating conditions.[150] Non-covalent binding of molecular catalysts, for instance through the preparation of inks with carbon-based materials, offers an alternative solution.[151,152] The use of organogels was recently reported for improving the stability of molecular photoanodes, while enabling permeation of the reactants to the surface.[153]

4. Electro-, photo-, and photoelectrocatalytic processes should consider suitable technologies for a sustained productivity of the desired chemicals, with the perspective of translating the system into real devices. In this sense, emerging technologies take advantage of gas diffusion electrodes, flow chemistry,[154] pulsed electrochemical techniques.[155] In the case of photocatalysis for water splitting, 100 m^2 wireless solar panels reactors were developed by Domen and co-workers and utilized for more than 1 year.[156]

5. "How far are electro- and photocatalysis from a real, industrial OAT application?" Some considerations can contribute to tracing hypothesis for the future. Currently, industrial electrochemical processes already operate on a large scale; in the chloralkali process (97 Mtons of Cl_2 produced in 2022), the electrolysis operates with a voltage of 3–3.2 V and at current densities of 3–4 kA·m^{-2} (i.e., 300–400 mA·cm^{-2}). Water electrolyzers operate at a lower voltage of 1.7–1.9 V at current densities around 1 kA·m^{-2}. Concerning electrosynthesis, one example in which a formal insertion of oxygen is involved is the electrooxidation of *p*-methoxytoluene to *p*-anisaldehyde developed by BASF (4–6 V, 30–50 mA·cm^{-2}, at 40°–50 °C in methanol).[157,158] Another advantage of electrochemical processes is the possibility to be powered with renewable energies, including photovoltaic panels; this is why electrochemical routes are considered as a viable possibility for application in carbon dioxide capture and reconversion.[159–161] Most of the industrial photocatalytic processes operate at a lower scale, take advantage of flow technology to allow a proper photon penetration,[154,162] and are focused in particular on the preparation of natural products and of derivatives for medicinal chemistry.[163–165]

Acknowledgments

Financial support by Italian Ministero dell'Università e della Ricerca (projects "PROMETEO" 2022KPK8WM to A.S.) and by the European Union – Next Generation UE (project "PHOTOCORE" P2022ZSPWF to A.S.) is acknowledged. Partial funding to A.A. and M.R. from Institut Universitaire de France (IUF) is warmly thanked. A.S. acknowledges the "Campagne d'invitations scientifiques 2024" of Université Paris Cité for funding a research visit in M.R.'s lab.

Conflict Interests

The authors declare no conflict of interest.

Data Availability Statement

The data that support the findings of this study are available from the corresponding author upon reasonable request.

Keywords: Catalysis • Electrochemistry • Industrial chemistry • Oxygen atom transfer • Photochemistry

[1] J. H. E. Teles, I. Ermans, G. Franz, R. A. Sheldon, *Oxidation* in *Ullmann's Encyclopedia of Industrial Chemistry* (Ed: B. Elvers), Wiley-VCH Verlag GmbH & Co. KGaA, Weinheim **2015**, pp. 1–103.
[2] R. W. Dugger, S. G. Ruggeri, J. A. Ragan, D. H. B. Ripin, *Chem. Rev.* **2006**, *106*, 2943–2989.
[3] J. R. Lockemeyer, T. L. Lohr, *ChemCatChem* **2023**, *15*, e202201511.
[4] T. L. Lohr, J. R. Lockemeyer, S. D. Bishopp, A. H. Motagamwala, G. J. Wells, T. Wermink, *Ind. Eng. Chem. Res.* **2024**, *63*, 18221–18240.
[5] R. G. Agarwal, S. C. Coste, B. D. Groff, A. M. Heuer, H. Noh, G. A. Parada, C. F. Wise, E. M. Nichols, J. J. Warren, J. M. Mayer, *Chem. Rev.* **2022**, *122*, 1–49.
[6] R. A. F. Tomás, J. C. M. Bordado, J. F. P. Gomes, *Chem. Rev.* **2013**, *113*, 7421–7469.
[7] A. Vomeri, M. Stucchi, A. Villa, C. Evangelisti, A. Beck, L. Prati, *J. Energy Chem.* **2022**, *70*, 45–51.
[8] H. Fujisaki, T. Ishizuka, H. Kotani, Y. Shiota, K. Yoshizawa, T. Kojima, *Nature* **2023**, *616*, 476–481.
[9] I. Schlichting, J. Berendzen, K. Chu, A. M. Stock, S. A. Maves, D. E. Benson, R. M. Sweet, D. Ringe, G. A. Petsko, S. G. Sligar, *Science* **2000**, *287*, 1615–1622.
[10] J. Rittle, M. T. Green, *Science* **2010**, *330*, 933–937.
[11] T. H. Yosca, J. Rittle, C. M. Krest, E. L. Onderko, A. Silakov, J. C. Calixto, R. K. Behan, M. T. Green, *Science* **2013**, *342*, 825–829.
[12] V. A. Larson, B. Battistella, K. Ray, N. Lehnert, W. Nam, *Nat. Rev. Chem.* **2020**, *4*, 404–419.
[13] X. Huang, J. T. Groves, *Chem. Rev.* **2018**, *118*, 2491–2553.
[14] A. Thibon, J. England, M. Martinho, V. G. Young, J. Frisch, R. Guillot, J.-J. Girerd, E. Munck, L. Que Jr., F. Banse, *Angew. Chem. Int. Ed.* **2008**, *47*, 7064–7067; *Angew. Chem.* **2008**, *120*, 7172–7175.
[15] M. Martinho, G. Blain, F. Banse, *Dalt. Trans.* **2010**, *39*, 1630–1634.
[16] J. R. Winkler, B. Gray, Harry, in *Mol. Electron. Struct. Transit. Met. Complexes I. Struct. Bond*. (Eds.: D. Mingos, P. Day, J. Dahl), Springer, Berlin, Heidelberg **2011**.
[17] L. Que, W. B. Tolman, *Nature* **2008**, *455*, 333–340.
[18] G. Li, A. K. Dilger, P. T. Cheng, W. R. Ewing, J. T. Groves, *Angew. Chem. Int. Ed.* **2017**, *57*, 1251–1255; *Angew. Chem.* **2017**, *130*, 1265–1269.
[19] S. R. Bell, J. T. Groves, *J. Am. Chem. Soc.* **2009**, *131*, 9640–9641.
[20] W. Nam, Y. M. Lee, S. Fukuzumi, *Acc. Chem. Res.* **2014**, *47*, 1146–1154.
[21] S. Fukuzumi, T. Kojima, Y. M. Lee, W. Nam, *Coord. Chem. Rev.* **2017**, *333*, 44–56.
[22] T. J. Collins, A. D. Ryabov, *Chem. Rev.* **2017**, *117*, 9140–9162.
[23] F. T. de Oliveira, A. Chanda, D. Benerjee, X. Shan, S. Mondal, L. Que, E. L. Bominaar, E. Munck, T. J. Collins, *Science* **2007**, *315*, 835–838.
[24] I. Prat, J. S. Mathieson, M. Guell, X. Ribas, J. M. Luis, L. Cronin, M. Costas, *Nat. Chem.* **2011**, *3*, 788–793.
[25] J. T. Groves, R. Quinn, *J. Am. Chem. Soc.* **1985**, *107*, 5790–5792.
[26] D. Di, J. Zhihui, L. Kang, L. Liao, X. Zhang, Y. Qiao, Y. Zhou, L. Yang, W. Binju, L. Aitao, *Nat. Catal.* **2025**, *8*, 20–32.
[27] A. Ourari, M. Khelafi, D. Aggoun, A. Jutand, C. Amatore, *Electrochim. Acta* **2012**, *75*, 366–370.
[28] T. V. Magdesieva, N. E. Borisova, A. V. Dolganov, Y. A. Ustynyuk, *Electrochim. Acta* **2012**, *85*, 475–485.
[29] Y. F. Tsai, T. Natarajan, Z. H. Lin, I. K. Tsai, D. Janmanchi, S. I. Chan, S. S. F. Yu, *J. Am. Chem. Soc.* **2022**, *144*, 9695–9706.
[30] S. E. Creager, S. A. Raybuck, R. W. Murray, *J. Am. Chem. Soc.* **1986**, *108*, 4225–4227.
[31] S. E. Creager, R. W. Murray, *Inorg. Chem.* **1987**, *26*, 2612–2618.
[32] P. Leduc, P. Battioni, J. F. Bartoli, D. Mansuy, *Tetrahedron Lett.* **1988**, *29*, 205–208.
[33] N. Kostopoulos, F. Banse, C. Fave, E. Anxolabéhere-Mallart, *Chem. Comm.* **2021**, *57*, 1198–1201.
[34] C. P. Horwitz, S. E. Creager, R. W. Murray, *Inorg. Chem.* **1990**, *29*, 1006–1011.
[35] J. C. Moutet, A. Ourari, *Electrochim. Acta* **1997**, *42*, 2525–2531.
[36] M. Xu, Q. He, X. Li, Y. Huang, Y. Weng, *ACS Catal.* **2025**, *15*, 3928–3939.
[37] P. Guo, K. Wong, *Electrochem. Comm.* **1999**, *1*, 559–563.
[38] P. Jego-Evanno, C. Moinet, G. Simonneaux, *C. R. Acad. Sci. Paris Ser. IIc Chim* **2000**, *3*, 711–716.
[39] A. L. Robinson, J.-N. Rebilly, R. Guillot, C. Herrero, H. Maisonneuve, F. Banse, *Chem. A Eur. J.* **2022**, *28*, e202200217.
[40] A. L. Robinson, E. Bannerman, R. Guillot, C. Herrero, K. Sénéchal-David, E. Rivière, F. Banse, J. N. Rebilly, *Eur. J. Inorg. Chem.* **2024**, *27*, e202300694.
[41] M. Mukherjee, A. Dey, *ACS Cent. Sci.* **2019**, *5*, 671–682.
[42] S. Samanta, S. Sengupta, S. Biswas, S. Ghosh, S. Barman, A. Dey, *J. Am. Chem. Soc.* **2023**, *145*, 26477–26486.
[43] M. Mukherjee, A. Dey, *Inorg. Chem.* **2020**, *59*, 7415–7425.
[44] R. Matheu, P. Garrido-Barros, M. Gil-Sepulcre, M. Z. Ertem, X. Sala, C. Gimbert-Suriñach, A. Llobet, *Nat. Rev. Chem.* **2019**, *3*, 331–341.
[45] J. D. Blakemore, R. H. Crabtree, G. W. Brudvig, *Chem. Rev.* **2015**, *115*, 12974–13005.
[46] M. M. T. Khan, G. Ramachandraiah, S. H. Mehata, *J. Mol. Catal.* **1989**, *50*, 123–129.
[47] J. T. Groves, J. A. Gilbert, *Inorg. Chem.* **1986**, *25*, 123–125.
[48] A. Das, J. E. Nutting, S. S. Stahl, *Chem. Sci.* **2019**, *10*, 7542–7548.
[49] B. Chandra, K. M. Hellan, S. Pattanayak, S. S. Gupta, *Chem. Sci.* **2020**, *11*, 11877–11885.
[50] S. S. Kim, S. Hong, A. Koovakattil Surendran, A. Roy, D. D. Malik, D. Chun, S. Kim, Y. Kim, Y.-M. Lee, Y. H. Lee, J. Roithová, S. H. Kim, W. Nam, K. Jin, *J. Am. Chem. Soc.* **2025**, *147*, 5269–5278.
[51] H. Tanaka, M. Kuroboshi, H. Takeda, H. Kanda, S. Torii, *J. Electroanal. Chem.* **2001**, *507*, 75–81.
[52] B. Lassalle-Kaiser, C. Hureau, D. A. Pantazis, Y. Pushkar, R. Guillot, V. K. Yachandra, J. Yano, F. Neese, E. Anxolabéhère-Mallart, *En. Environ. Sci.* **2010**, *3*, 924–938.
[53] M. A. Hoque, T. Jiang, D. L. Poole, S. S. Stahl, *J. Am. Chem. Soc.* **2024**, *146*, 21960–21967.
[54] M. A. Hoque, J. B. Gerken, S. S. Stahl, *Science* **2024**, *383*, 173–178.
[55] B. Mühldorf, U. Lennert, R. Wolf, *Phys. Sci. Rev.* **2019**, *4*, 20180030.
[56] C. Yang, H. Wang, P. Xie, *ChemSusChem* **2025**, *18*, e202401915.
[57] L. Schneider, Y. Mekmouche, P. Rousselot-Pailley, A. J. Simaan, V. Robert, M. Reglier, A. Aukauloo, T. Tron, *ChemSusChem* **2015**, *8*, 3048–3051.
[58] D. Chao, M. Zhao, *ChemSusChem* **2017**, *10*, 3358–3362.
[59] J. Klein, A. Girardon, A. Moreno Betancourt, F. Loiseau, D. Jouvenot, J. Pecaut, O. Hamelin, S. Torelli, *Eur. J. Inorg. Chem.* **2023**, *26*, e202300397.
[60] O. Hamelin, P. Guillo, F. Loiseau, M.-F. Boissonnet, S. Ménage, *Inorg. Chem.* **2011**, *50*, 7952–7954.
[61] R. Zhang, R. E. P. Chandrasena, E. Martinez, J. H. Horner, M. Newcomb, *Org. Lett.* **2005**, *7*, 1193–1195.
[62] D. N. Harischandra, R. Zhang, M. Newcomb, *J. Am. Chem. Soc.* **2005**, *127*, 13776–13777.

[63] S. L. Esarey, J. C. Holland, B. M. Bartlett, *Inorg. Chem.* **2016**, *55*, 11040–11049.
[64] O. Cusso, I. Garcia-Bosch, X. Ribas, J. Lloret-Fillol, M. Costas, *J. Am. Chem. Soc.* **2013**, *135*, 14871–14878.
[65] G. P. Van Trieste, J. H. Reibenspies, Y. S. Chen, D. Sengupta, R. R. Thompson, D. C. Powers, *Chem. Comm.* **2022**, *364*, 12608–12611.
[66] J. Rosenthal, B. J. Pistorio, L. L. Chng, D. G. Nocera, *J. Org. Chem.* **2005**, *70*, 1885–1888.
[67] J. Rosenthal, T. D. Luckett, J. M. Hodgkiss, D. G. Nocera, *J. Am. Chem. Soc.* **2006**, *128*, 6546–6547.
[68] D. N. Harischandra, G. Lowery, R. Zhang, M. Newcomb, *Org. Lett.* **2009**, *11*, 2089–2092.
[69] *Flavin-Based Catalysis – Principles and Applications* (Eds.: R. Cibulka, M. Fraaije), Wiley-VCH GmbH & Co. KGaA, Weinheim, **2021**, pp. 1–323.
[70] S. Fukuzumi, K. Yasui, T. Suenobu, K. Ohkubo, M. Fujitsuka, O. Ito, *J. Phys. Chem.* **2001**, *105*, 10501–10510.
[71] A. H. Tolba, F. Vavra, J. Chudoba, R. Cibulka, *Eur. J. Org. Chem.* **2020**, *2020*, 1579–1585.
[72] S. Jiri, H. Schmaderer, B. Konig, *Chem. A Eur. J.* **2008**, *14*, 1854–1865.
[73] R. Lechner, S. Kümmel, B. König, *Photochem. Photobiol. Sci.* **2010**, *9*, 1367–1377.
[74] J. L. Fillol, Z. Codolà, I. Garcia-Bosch, L. Gàmez, J. J. Pla, M. Costas, *Nat. Chem.* **2011**, *3*, 807–813.
[75] I. Prat, J. S. Mathieson, M. Güell, X. Ribas, J. M. Luis, L. Cronin, M. Costas, *Nat. Chem.* **2011**, *3*, 788–793.
[76] B. Mühldorf, R. Wolf, *Angew. Chem. Int. Ed.* **2016**, *55*, 427–430; *Angew. Chem.* **2016**, *128*, 437–441.
[77] F. Avenier, C. Herrero, W. Leibl, A. Desbois, R. Guillot, J.-P. Mahy, A. Aukauloo, *Angew. Chem. Int. Ed.* **2013**, *125*, 3722–3725; *Angew. Chem.* **2013**, *125*, 3722–3725.
[78] M. E. Ener, Y. T. Lee, J. R. Winkler, H. B. Gray, L. Cheruzel, *Proc. Nat. Acad. Sci.* **2010**, *107*, 18783–18786.
[79] W. Iali, P. H. Lanoe, S. Torelli, D. Jouvenot, F. Loiseau, C. Lebrun, O. Hamelin, S. Ménage, *Angew. Chem. Int. Ed.* **2015**, *54*, 8415–8419; *Angew. Chem.* **2015**, *127*, 8535–8539.
[80] N. T. Vo, Y. Mekmouche, T. Tron, R. Guillot, F. Banse, Z. Halime, M. Sircoglou, W. Leibl, A. Aukauloo, *Angew. Chem. Int. Ed.* **2019**, *58*, 16023–16027; *Angew. Chem.* **2019**, *131*, 16169–16173.
[81] E. Pugliese, N. T. Vo, A. Boussac, F. Banse, Y. MekMouche, J. Simaan, T. Tron, P. Gotico, M. Sircoglou, Z. Halime, W. Leibl, A. Aukauloo, *Chem. Sci.* **2022**, *13*, 12332–12339.
[82] A. C. Maliyackel, J. W. Otvos, L. Spreert, M. Calvin, *Proc. Nat. Acad. Sci.* **1986**, *83*, 3572–3574.
[83] S. Fukuzumi, T. Kishi, H. Kotani, Y.-M. Lee, W. Nam, *Nat. Chem.* **2011**, *3*, 38–41.
[84] B. Chandra, K. K. Singh, S. S. Gupta, *Chem. Sci.* **2017**, *8*, 7545–7551.
[85] F. T. De Oliveira, A. Chanda, D. Banerjee, X. Shan, S. Mondal, L. Que, E. L. Bominaar, E. Münck, T. J. Collins, *Science* **2007**, *315*, 835–838.
[86] T. J. Collins, *Acc. Chem. Res.* **2002**, *35*, 782–790.
[87] H. Kotani, T. Suenobu, Y. Lee, W. Nam, S. Fukuzumi, *J. Am. Chem. Soc.* **2011**, *133*, 3249–3251.
[88] A. Company, G. Sabenya, M. Gonzalez-Béjar, L. Gomez, M. Clemancey, G. Blondin, A. J. Jansienwski, M. Puri, W. R. Browne, J.-M. Latour, L. Que, M. Costas, J. Perez-Prieto, J. Loret-Fillol, *J. Am. Chem. Soc.* **2014**, *136*, 4624–4633.
[89] C. Herrero, A. Quaranta, M. Sircoglou, K. Sénéchal-David, A. Baron, I. M. Marín, C. Buron, J.-P. Baltaze, W. Leibl, A. Aukauloo, F. Banse, *Chem. Sci.* **2015**, *6*, 2323–2327.
[90] J. W. Han, J. Jung, Y. M. Lee, W. Nam, S. Fukuzumi, *Chem. Sci.* **2017**, *8*, 7119–7125.
[91] B. An, Z. Li, Z. Wang, X. Zeng, X. Han, Y. Cheng, A. M. Sheveleva, Z. Zhang, F. Tuna, E. J. L. McInnes, M. D. Frogley, A. J. Ramirez-Cuesta, L. S. Natrajan, C. Wang, W. Lin, S. Yang, M. Schröder, *Nat. Mater.* **2022**, *21*, 932–938.
[92] T. Dreher, L. Geciauskas, S. Steinfeld, B. Procacci, A. C. Whitwood, J. M. Lynam, R. E. Douthwaite, A.-K. Duhme-Klair, *Chem. Sci.* **2024**, *15*, 16186–16195.
[93] N. J. Castellanos, H. Martínez Q, F. Martínez O, K. Leus, P. Van Der Voort, *Res. Chem. Intermed.* **2021**, *47*, 4227–4244.
[94] J. Wang, S. Qiao, M. Yang, Z. Guo, *Small* **2025**, *21*, 2409292.
[95] M. J. Katz, S. C. Riha, N. C. Jeong, A. B. F. Martinson, O. K. Farha, J. T. Hupp, *Coord. Chem. Rev.* **2012**, *256*, 2521–2529.
[96] K. Sivula, F. Le Formal, M. Grätzel, *ChemSusChem* **2011**, *4*, 432–449.
[97] N. Dalle Carbonare, V. Cristino, S. Berardi, S. Carli, R. Argazzi, S. Caramori, L. Meda, A. Tacca, C. A. Bignozzi, *ChemPhysChem* **2014**, *15*, 1164–1174.
[98] T. Li, T. Kasahara, J. He, K. E. Dettelbach, G. M. Sammis, C. P. Berlinguette, *Nat. Commun.* **2017**, *8*, 390.
[99] H. Tateno, S. Iguchi, Y. Miseki, K. Sayama, *Angew. Chem. Int. Ed.* **2018**, *57*, 11238–11241; *Angew. Chem.* **2018**, *130*, 11408–11411.
[100] H. Tateno, S. Y. Chen, Y. Miseki, T. Nakajima, T. Mochizuki, K. Sayama, *ACS Sustainable Chem. Eng.* **2022**, *10*, 7586–7594.
[101] Y. Yang, G. A. Volpato, E. Rossin, N. Peruffo, F. Tumbarello, C. Nicoletti, R. Bonetto, L. Paoloni, P. Umari, E. Colusso, L. Dell'Amico, S. Berardi, E. Collini, S. Caramori, S. Agnoli, A. Sartorel, *ChemSusChem* **2023**, *16*, e202201980.
[102] T. K. Liu, G. Y. Jang, S. Kim, K. Zhang, X. Zheng, J. H. Park, *Small Methods* **2024**, *8*, 2300315.
[103] Y. Zhao, C. Deng, D. Tang, L. Ding, Y. Zhang, H. Sheng, H. Ji, W. Song, W. Ma, C. Chen, J. Zhao, *Nat. Catal.* **2021**, *4*, 684–691.
[104] C. J. Seel, T. Gulder, *ChemBioChem* **2019**, *20*, 1871–1897.
[105] J. Jang, W. A. Khan, F. Hollmann, K. Won, C. B. Park, *ACS Sustainable Chem. Eng.* **2024**, *12*, 8950–8957.
[106] Y. Liu, L. Zuo, Q. Lv, B. Yu, *Curr. Opin. Green Sustain. Chem.* **2023**, *40*, 100759.
[107] F. Valentini, V. Conte, P. Galloni, F. Sabuzi, *Catalysts* **2023**, *13*, 220.
[108] A. Vega-Peñaloza, J. Mateos, X. Companyó, M. Escudero-Casao, L. Dell'Amico, *Angew. Chem. Int. Ed.* **2021**, *60*, 1082–1097; *Angew. Chem.* **2021**, *133*, 1096–1111.
[109] T. Shiragami, K. Kubomura, D. Ishibashi, H. Inoue, *J. Am. Chem. Soc.* **1996**, *118*, 6311–6312.
[110] S. Mathew, F. Kuttassery, Y. Gomi, D. Yamamoto, R. Kiyooka, S. Onuki, Y. Nabetani, H. Tachibana, H. Inoue, *J. Photochem. Photobiol. A Chem.* **2015**, *313*, 137–142.
[111] F. Kuttassery, S. Mathew, S. N. Remello, A. Thomas, K. Sano, Y. Ohsaki, Y. Nabetani, H. Tachibana, H. Inoue, *Coord. Chem. Rev.* **2018**, *377*, 64–72.
[112] I. Guerrero, C. Viñas, I. Romero, F. Teixidor, *Green Chem.* **2021**, *23*, 10123–10131.
[113] C. K. Spyropoulou, E. Skolia, D. F. Flesariu, G. A. Zissimou, P. L. Gkizis, I. Triandafillidi, M. Athanasiou, G. Itskos, P. A. Koutentis, C. G. Kokotos, *Adv. Synth. Catal.* **2023**, *365*, 2643–2650.
[114] Q. Qin, L. Zhang, J. Wei, X. Qiu, S. Hao, X.-D. An, N. Jiao, *Nat. Commun.* **2024**, *15*, 9015.
[115] D. M. Jerina, D. R. Boyd, J. W. Daly, *Tetrahedron Lett.* **1970**, *11*, 457–460.
[116] M. Sako, K. Shimada, K. Hirota, Y. Maki, *J. Am. Chem. Soc.* **1986**, *108*, 6039–6041.
[117] A. Petrosyan, R. Hauptmann, J. Pospech, *European J. Org. Chem.* **2018**, *2018*, 5237–5252.
[118] C. Y. Cai, S. J. Chen, R. R. Merchant, Y. Kanda, T. Qin, *J. Am. Chem. Soc.* **2024**, *146*, 24257–24264.

[119] K. Ohkubo, T. Kobayashi, S. Fukuzumi, *Angew. Chem. Int. Ed.* **2011**, *50*, 8652–8655; *Angew. Chem.* **2011**, *123*, 8811–8814.
[120] K. Ohkubo, A. Fujimoto, S. Fukuzumi, *J. Am. Chem. Soc.* **2013**, *135*, 5368–5371.
[121] H. Huang, T. H. Lambert, *Angew. Chem. Int. Ed.* **2021**, *60*, 11163–11167; *Angew. Chem.* **2021**, *133*, 11263–11267.
[122] S. Bhuyan, A. Gogoi, J. Basumatary, B. Gopal Roy, *Eur. J. Org. Chem.* **2022**, *2022*, e202200148.
[123] E. Tacchi, G. Rossi, M. Natali, L. Đordevic, A. Sartorel, *Adv. Sustain. Syst.* **2024**, *9*, 2400538.
[124] D. Jiang, Q. Zhang, L. Yang, Y. Deng, B. Yang, Y. Liu, C. Zhang, *Renew. Energy* **2021**, *174*, 928–938.
[125] H. Asahara, Y. Horikawa, K. Iwai, N. Nishiwaki, *J. Photochem. Photobiol.* **2023**, *15*, 100184.
[126] K. Ohkubo, A. Fujimoto, S. Fukuzumi, *Chem. Commun.* **2011**, *47*, 8515–8517.
[127] M. Uygur, J. H. Kuhlmann, M. C. Pérez-Aguilar, D. G. Piekarski, O. G. Mancheño, *Green Chem.* **2021**, *23*, 3392–3399.
[128] B. Worp, V. Der Alexander, T. Ritter, *J. Am. Chem. Soc.* **2025**, *147*, 4736–4742.
[129] A. L. De Abreu, D. Taton, D. M. Bassani, *Angew. Chem. Int. Ed.* **2025**, *64*, e202418680; *Angew. Chem.* **2025**, *137*, e202418680.
[130] C. Ascenzi Pettenuzzo, D. Ranjan Pradhan, J. Singh, L. Liu, G. Cuffel, M. J. Vetticatt, Y. Deng, *J. Am. Chem. Soc.* **2025**, *147*, 10382–10390.
[131] H. Huang, K. A. Steiniger, T. H. Lambert, *J. Am. Chem. Soc.* **2022**, *144*, 12567–12583.
[132] J. Žurauskas, S. Boháčová, S. Wu, V. Butera, S. Schmid, M. Domański, T. Slanina, J. P. Barham, *Angew. Chem. Int. Ed.* **2023**, *62*, e202307550; *Angew. Chem.* **2023**, *135*, e202307550.
[133] M. C. Lamb, K. A. Steiniger, L. K. Trigoura, J. Wu, G. Kundu, H. Huang, T. H. Lambert, *Chem. Rev.* **2024**, *124*, 12264–12304.
[134] H. Huang, Z. M. Strater, M. Rauch, J. Shee, T. J. Sisto, C. Nuckolls, T. H. Lambert, *Angew. Chem. Int. Ed.* **2019**, *59*, 13318–13322; *Angew. Chem.* **2019**, *131*, 13452–13456.
[135] H. Huang, T. H. Lambert, *J. Am. Chem. Soc.* **2021**, *143*, 7247–7252.
[136] T. Shen, Y. Li, K. Ye, T. H. Lambert, *Nature* **2023**, *614*, 275–281.
[137] H. Huang, T. H. Lambert, *J. Am. Chem. Soc.* **2022**, *144*, 18803–18809.
[138] L. Quan, H. Jiang, G. Mei, Y. Sun, B. You, *Chem. Rev.* **2024**, *124*, 3894–3812.
[139] P. Franceschi, E. Rossin, G. Goti, A. Scopano, A. Vega-Penaloza, M. Natali, D. Singh, A. Sartorel, L. Dell'Amico, *J. Org. Chem.* **2023**, *88*, 6454–6464.
[140] L. Fortier, C. Lefebvre, N. Hoffmann, *Beilstein J. Org. Chem.* **2025**, *21*, 296–326.
[141] D. Mazzarella, C. Qi, M. Vanzella, A. Sartorel, G. Pelosi, L. Dell'Amico, *Angew. Chem. Int. Ed.* **2024**, *63*, e202401361; *Angew. Chem.* **2024**, *136*, e202401361.
[142] J. Z. Zhang, E. Reisner, *Nat. Rev. Chem.* **2020**, *4*, 6–21.
[143] J. D. Megiatto, D. D. Méndez-Hernández, M. E. Tejeda-Ferrari, A. L. Teillout, M. J. Llansola-Portolés, G. Kodis, O. G. Poluektov, T. Rajh, V. Mujica, T. L. Groy, D. Gust, T. A. Moore, A. L. Moore, *Nat. Chem.* **2014**, *6*, 423–428.
[144] X. Cao, Z. Chen, R. Lin, W.-C. Cheong, S. Liu, J. Zhang, Q. Peng, C. Chen, T. Han, X. Tong, Y. Wang, R. Shen, W. Zhu, D. Wang, Y. Li, *Nat. Catal.* **2018**, *1*, 704–710.
[145] W. R. Leow, Y. Lum, A. Ozden, Y. Wang, D.-H. Nam, B. Chen, J. Wicks, T.-T. Zhuang, F. Li, D. Sinton, E. H. Sargent, *Science* **2020**, *368*, 1228–1233.
[146] Z. Mi, Y. Li, C. Wu, M. Zhang, X. Cao, S. Xi, J. Zhang, W. R. Leow, *Nat. Commun.* **2025**, *16*, 3424.
[147] Y. Yang, X. Yang, L. Tang, S. Sung, Z. Wang, Z. Lu, S. H. Oh, Q. Zhong, J. H. Park, K. Zhang, *Adv. Mater.* **2025**, *37*, 2502321.
[148] Y. Yang, X. Yuan, Q. Wang, S. Wan, C. Lin, S. Lu, Q. Zhong, K. Zhang, *Angew. Chem. Int. Ed.* **2024**, *63*, e202314383; *Angew. Chem.* **2024**, *136*, e202314383.
[149] X. Liu, Z. Chen, S. Xu, G. Liu, Y. Zhu, X. Yu, L. Sun, F. Li, *J. Am. Chem. Soc.* **2022**, *144*, 19770–19777.
[150] K. L. Materna, R. H. Crabtree, G. W. Brudvig, *Chem. Soc. Rev.* **2017**, *46*, 6099–6110.
[151] S. Ren, D. Joulié, D. Salvatore, K. Torbensen, M. Wang, M. Robert, C. P. Berlinguette, *Science* **2019**, *365*, 367–369.
[152] M. Wang, K. Torbensen, D. Salvatore, S. Ren, D. Joulié, F. Dumoulin, D. Mendoza, B. Lassalle-Kaiser, U. Işci, C. P. Berlinguette, M. Robert, *Nat. Commun.* **2019**, *10*, 3602.
[153] D. Bruggeman, A. Laoprte, R. J. Detz, S. Mathew, J. N. H. Reek, *Angew. Chem. Int. Ed.* **2022**, *61*, e202200175; *Angew. Chem.* **2022**, *134*, e202200175.
[154] L. Buglioni, F. Raymenants, A. Slattery, S. D. A. Zondag, T. Noël, *Chem. Rev.* **2022**, *122*, 2752–2906.
[155] X. Wang, M. Jiang, P. Yang, H. Zhou, W. Xi, J. Duan, M. Ratova, D. Wu, X. Jiang, *Surf. Interf.* **2024**, *50*, 104519.
[156] H. Nishiyama, T. Yamada, M. Nakabayashi, Y. Maehara, M. Yamaguchi, Y. Kuromiya, Y. Nagatsuma, H. Tokudome, S. Akiyama, T. Watanabe, R. Narushima, S. Okunaka, N. Shibata, T. Takata, T. Hisatomi, K. Domen, *Nature* **2021**, *598*, 304–307.
[157] M. C. Leech, A. D. Garcia, A. Petti, A. P. Dobbs, K. Lam, *React. Chem. Eng.* **2020**, *5*, 977–990.
[158] D. Lehnherr, L. Chen, *Org. Proc. Res. Dev.* **2024**, *28*, 338–366.
[159] T. Lu, T. Xu, S. Zhu, J. Li, J. Wang, H. Jin, X. Wang, J. J. Lv, Z. J. Wang, S. Wang, *Adv. Mater.* **2023**, *35*, 1–18.
[160] T. L. Biel-Nielsen, T. A. Hatton, S. N. Villadsen, J. S. Jakobsen, J. L. Bonde, A. M. Spormann, P. L. Fosbol, *ChemSusChem* **2023**, *16*, e202202345.
[161] S. Varhade, A. Guruji, C. Singh, G. Cicero, M. García-Melchor, J. Helsen, D. Pant, *ChemElectroChem* **2025**, *12*, 202400512.
[162] E. Kayahan, M. Jacobs, L. Braeken, L. C. J. Thomassen, S. Kuhn, T. Van Gerven, M. E. Leblebici, *Beilstein J. Org. Chem.* **2020**, *16*, 2484–2504.
[163] L. Candish, K. D. Collins, G. C. Cook, J. J. Douglas, A. Gómez-Suárez, A. Jolit, S. Keess, *Chem. Rev.* **2022**, *122*, 2907–2980.
[164] E. G. Moschetta, G. C. Cook, L. J. Edwards, M. A. Ischay, Z. Lei, F. Buono, F. Lévesque, J. A. O. Garber, M. MacTaggart, M. Sezen-Edmonds, K. P. Cole, M. G. Beaver, J. Doerfler, S. M. Opalka, W. Liang, P. D. Morse, N. Miyake, *Org. Process Res. Dev.* **2024**, *28*, 831–846.
[165] M. H. Shaw, J. Twilton, D. W. C. MacMillan, *J. Org. Chem.* **2016**, *81*, 6898–6926.

Manuscript received: May 05, 2025
Revised manuscript received: May 29, 2025